

1 **Title:** Six decades of losses and gains in alpha diversity of European plant communities

2 **Running title:** Interpolation of species richness dynamics

3 **Keywords:** alpha diversity, autocorrelation, biogeographic regions, habitat specificity, latitudinal  
4 gradient, machine learning, nature conservation, random forests, statistical interpolation,  
5 vegetation resurvey

6 **Authors:** Gabriele Midolo<sup>1\*</sup>, Adam Thomas Clark<sup>2</sup>, Milan Chytrý<sup>3</sup>, Franz Essl<sup>4</sup>, Stefan  
7 Dullinger<sup>5</sup>, Ute Jandt<sup>6,7</sup>, Helge Bruelheide<sup>6,7</sup>, Olivier Argagnon<sup>8</sup>, Idoia Biurrun<sup>9</sup>, Alessandro  
8 Chiarucci<sup>10</sup>, Renata Čušterevska<sup>11</sup>, Pieter De Frenne<sup>12</sup>, Michele De Sanctis<sup>13</sup>, Jürgen Dengler<sup>14,15</sup>,  
9 Jan Divíšek<sup>3</sup>, Tetiana Dziuba<sup>16</sup>, Rasmus Ejrnæs<sup>17</sup>, Emmanuel Garbolino<sup>18</sup>, Estela Illa<sup>19,20</sup>, Anke  
10 Jentsch<sup>15,21</sup>, Borja Jiménez-Alfaro<sup>22</sup>, Jonathan Lenoir<sup>23</sup>, Jesper Erenskjold Moeslund<sup>17</sup>, Francesca  
11 Napoleone<sup>13</sup>, Remigiusz Pielech<sup>24</sup>, Sabine B. Rumpf<sup>25</sup>, Irati Sanz-Zubizarreta<sup>9</sup>, Vasco Silva<sup>26</sup>,  
12 Jens-Christian Svenning<sup>27</sup>, Grzegorz Swacha<sup>28</sup>, Martin Večeřa<sup>3</sup>, Denys Vynokurov<sup>6,7,16</sup>, Petr  
13 Keil<sup>1</sup>

14 **Affiliations:**

15 1: Department of Spatial Sciences, Faculty of Environmental Sciences, Czech University of Life  
16 Sciences Prague, Praha-Suchdol, Czech Republic

17 2: Department of Biology, University of Graz, Graz, Austria

18 3: Department of Botany and Zoology, Faculty of Science, Masaryk University, Brno, Czech  
19 Republic

20 4: Division of BioInvasions, Global Change & Macroecology, Department of Botany and  
21 Biodiversity Research, University of Vienna, Vienna, Austria

22 5: Division of Biodiversity Dynamics and Conservation, Department of Botany and Biodiversity  
23 Research, University Vienna, Vienna, Austria

24 6: Institute of Biology/Geobotany and Botanical Garden, Martin Luther University Halle-  
25 Wittenberg, Halle, Germany

26 7: German Centre for Integrative Biodiversity Research (iDiv) Halle-Jena-Leipzig, Leipzig,  
27 Germany

28 8: Conservatoire Botanique National Méditerranéen, Hyères, France

29 9: Department of Plant Biology and Ecology, Faculty of Science and Technology, University of  
30 the Basque Country UPV/EHU, Bilbao, Spain

31 10: BIOME Lab, Department of Biological, Geological and Environmental Sciences, Alma  
32 Mater Studiorum – University of Bologna, Bologna, Italy

33 11: Faculty of Natural Sciences and Mathematics, Ss. Cyril and Methodius University, Skopje,  
34 North Macedonia

35 12: Forest & Nature Lab, Faculty of Bioscience Engineering, Ghent University, Gontrode,  
36 Belgium

37 13: Department of Environmental Biology, Sapienza University of Rome, Rome, Italy

38 14: Vegetation Ecology Research Group, Institute of Natural Resource Sciences (IUNR), Zurich  
39 University of Applied Sciences (ZHAW), Wädenswil, Switzerland

40 15: Bayreuth Center of Ecology and Environmental Research (BayCEER), University of  
41 Bayreuth, Bayreuth, Germany

42 16: Department of Geobotany and Ecology, M.G. Kholodny Institute of Botany, National  
43 Academy of Sciences of Ukraine, Kyiv, Ukraine

44 17: Department of Ecoscience, Aarhus University, Aarhus, Denmark

45 18: ISIGE, MINES Paris PSL, Fontainebleau, France

46 19: Departament de Biologia Evolutiva, Ecologia i Ciències Ambientals, Facultat de Biologia,  
47 Universitat de Barcelona, Barcelona, Spain

48 20: Institut de Recerca de la Biodiversitat (IRBio), Universitat de Barcelona, Barcelona, Spain

49 21: Disturbance Ecology and Vegetation Dynamics, University of Bayreuth, Bayreuth, Germany

50 22: Biodiversity Research Institute (IMIB), University of Oviedo-CSIC-Principality of Asturias,  
51 Oviedo, Spain

52 23: UMR CNRS 7058 Ecologie et Dynamique des Systèmes Anthropisés (EDYSAN), Université  
53 de Picardie Jules Verne, Amiens, France

54 24: Institute of Botany, Faculty of Biology, Jagiellonian University, Kraków, Poland

55 25: Department of Environmental Sciences, University of Basel, Basel, Switzerland

56 26: Egas Moniz Center for Interdisciplinary Research (CiiEM), Egas Moniz School of Health  
57 and Science, Caparica, Portugal

58 27: Center for Ecological Dynamics in a Novel Biosphere (ECONOVO), Department of Biology,  
59 Aarhus University, Aarhus, Denmark

60 28: Botanical Garden, University of Wrocław, Wrocław, Poland

61 **Corresponding author:**

62 \* Gabriele Midolo

63 e-mail: [midolo@fzp.czu.cz](mailto:midolo@fzp.czu.cz); phone: 0039 3703185439

64 Address: Faculty of Environmental Sciences, Czech University of Life Sciences Prague,

65 Kamýcká 129, 165 00 Praha – Suchdol

66 ORCID: <https://orcid.org/0000-0003-1316-2546>

67 **Statement of authorship:** G.M. and P.K. developed the original idea and conceptualized the  
68 methodology. G.M. led the investigation, data processing, visualizations, analysis, drafted the  
69 original manuscript, and led the writing. P.K. supervised the project and contributed to the  
70 original draft. P.K., A.T.C, and F.E. acquired funding. All authors except G.M., A.T.C., and P.K.  
71 contributed the data used in the analysis. All authors reviewed the manuscript.

72 **Data accessibility statement:** The data and R code to fully reproduce the analyses are available  
73 in the GitHub repository: [https://github.com/gmidolo/interpolated\\_S\\_change](https://github.com/gmidolo/interpolated_S_change). Output files  
74 including model fits are available on Zenodo: <https://doi.org/10.5281/zenodo.15836616>. An  
75 interactive map exploring interpolated spatiotemporal changes in species richness can be  
76 accessed at: [https://gmidolo.shinyapps.io/interpolated\\_s\\_change\\_app](https://gmidolo.shinyapps.io/interpolated_s_change_app) (GitHub repository:  
77 [https://github.com/gmidolo/interpolated\\_S\\_change\\_app](https://github.com/gmidolo/interpolated_S_change_app)). The use of the data for additional  
78 publications, and the access to complete and original vegetation data, are only possible through a  
79 request to EVA Coordinating Board (see <https://euroveg.org/eva-database/>).

## 80 **Abstract**

81 Biodiversity change forecasts rely on long-term time series, but such data are often scarce in  
82 space and time. Here, we interpolated spatiotemporal changes in species richness using a novel  
83 machine learning method without requiring temporal replication at sites. Using 698,692 one-time  
84 survey vegetation plots, we estimated trends in vascular plant alpha diversity across Europe from  
85 1960 to 2020 and validated our approach against 22,852 independent time series. We found an  
86 overall near-zero net change in species richness. However, species richness generally declined  
87 from 1960 to 1980 across habitats, followed by an increase from 2000 to 2020. Declines were  
88 most pronounced in forests, but trends varied significantly across habitats and regions, with  
89 overall increases at higher latitudes and elevations, and declines or stable trends elsewhere. Our  
90 findings demonstrate how data without temporal replication can be used to reveal context-  
91 dependent biodiversity dynamics, underscoring the importance of such forecasts for conservation  
92 and management.

## 93 **1. Introduction**

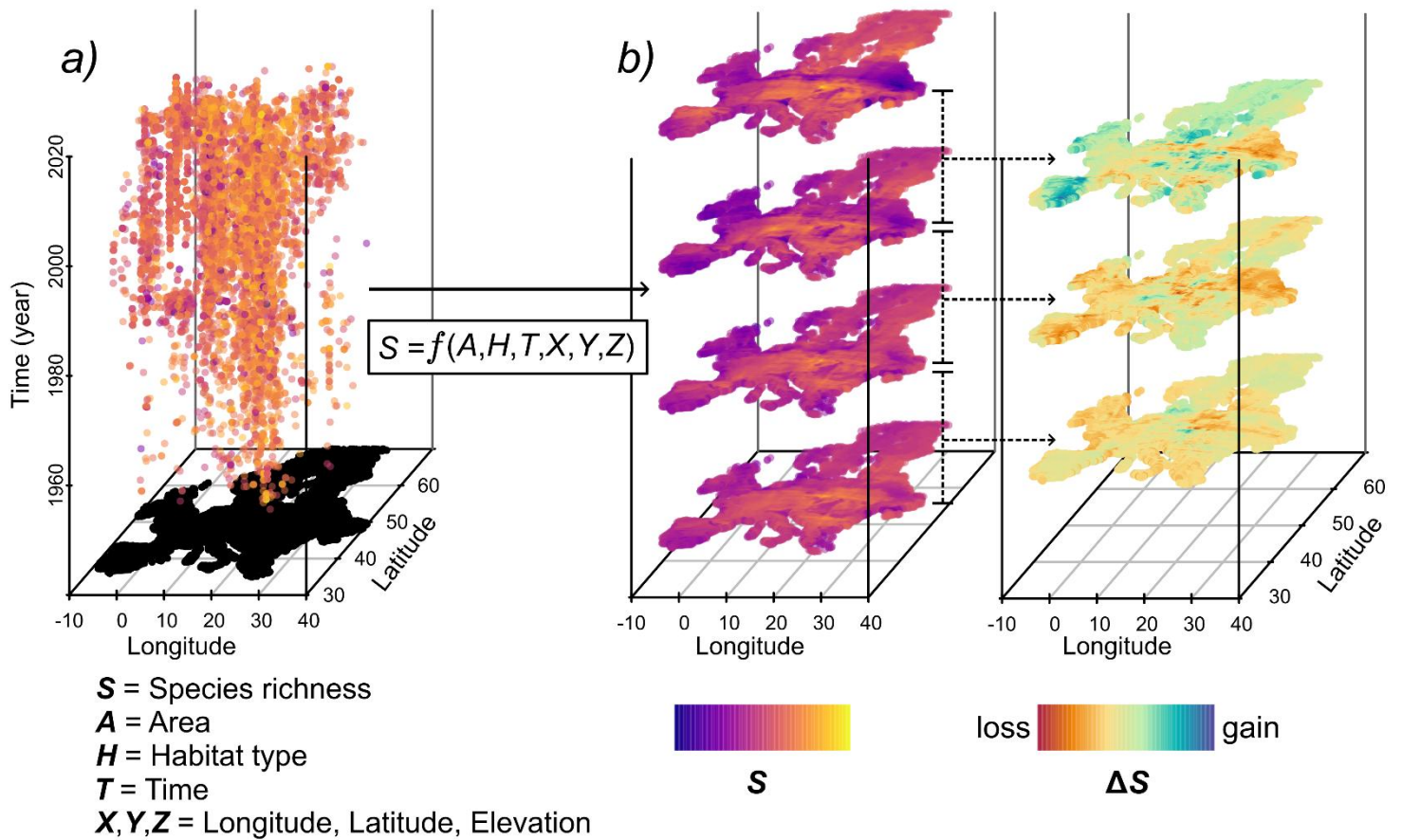
94 Humans are driving major biodiversity changes worldwide (Díaz *et al.* 2019; IPBES 2019), but  
95 the magnitude of these changes remains poorly understood across most taxa, regions, and scales  
96 (Gonzalez *et al.* 2016; Johnson *et al.* 2024). At the finest grain, that of the local biological  
97 community, losses and gains often offset each other (Bernhardt-Römermann *et al.* 2015; Blowes  
98 *et al.* 2019; Dornelas *et al.* 2014; Jandt *et al.* 2022; Klinkovská *et al.* 2025; Pilotto *et al.* 2020;  
99 Vellend *et al.* 2013). In Europe, trends in plant diversity at the community level have been  
100 differentially impacted by various causes, such as agricultural intensification, biological  
101 invasions, climate change, conservation measures, and eutrophication (Finderup Nielsen *et al.*  
102 2021; Gray *et al.* 2016; Steinbauer *et al.* 2018; Stevens *et al.* 2010; Vellend *et al.* 2017; Vilà *et*

103 *al.* 2011). The relative strength of these drivers potentially varies over different historical periods  
104 (Klinkovská *et al.* 2024; Wesche *et al.* 2012), and their impacts may lag in time and only unfold  
105 after many decades (Dullinger *et al.* 2013). Consequently, the magnitude and direction of plant  
106 diversity change can differ across biogeographical regions and habitat types (Blowes *et al.* 2019;  
107 Pilotto *et al.* 2020). This wide variety of trends calls for time-series analyses capable of  
108 identifying fine-grain temporal changes in plant biodiversity across large spatiotemporal extents.  
109 To quantify plant diversity trends, considerable efforts are underway to resurvey vegetation plots  
110 across Europe (Jandt *et al.* 2022; Klinkovská *et al.* 2025), which recently culminated into  
111 ReSurveyEurope (Knollová *et al.* 2024), a database collating thousands of vegetation plot  
112 observations from numerous resurvey and monitoring projects. Despite the impressive collective  
113 effort and the extensive data now available, this database has significant geographical gaps, is  
114 biased toward well-preserved habitats and sites, becomes increasingly sparse further back in  
115 time, and varies in the length of observation intervals between surveys – with a large fraction of  
116 vegetation plots resurveyed only once. Furthermore, trends in plant alpha diversity derived from  
117 resurvey studies are potentially sensitive to plot relocation and observer error (Boch *et al.* 2022;  
118 Klinkovská *et al.* 2025; Verheyen *et al.* 2018). As a result, we still have limited knowledge of  
119 how plant diversity at the community level (i.e., alpha diversity) has changed across various  
120 European biogeographical regions and habitats.

121 To address data gaps in space and time, we employ a novel machine learning approach (Keil &  
122 Chase 2022) to interpolate temporal biodiversity change using only *static* data, namely data  
123 without temporal replication at any given site. Our approach relies on the well-established fact  
124 that biodiversity is spatially (Legendre 1993; Tobler 1970) and temporally (Dornelas *et al.* 2013)  
125 *autocorrelated*, which is caused by the continuity of species distributions across space and time

126 due to dispersal limitation and environmental structure (Dornelas *et al.* 2013). Because of this  
127 autocorrelation, we propose that biodiversity can be interpolated jointly in space and time [i.e., in  
128 the *space-time cube* (Mahecha *et al.* 2020)] (**Figure 1**). Specifically, we employed Random  
129 Forests (Breiman 2001; Wright & Ziegler 2017) to interpolate community-level plant diversity in  
130 a multidimensional domain defined by geographical coordinates and time, while also accounting  
131 for the effect of varying plot area on species richness estimates (Dengler *et al.* 2020; Storch  
132 2016). Our approach provides predictions of plant diversity within the temporal dimension,  
133 ultimately representing *interpolated time series* of biodiversity change.

134 To this end, we utilized 698,692 static vegetation plots the European Vegetation Archive (EVA)  
135 (Chytrý *et al.* 2016) and ReSurveyEurope (Knollová *et al.* 2024), sampled between 1945 and  
136 2023 with plot sizes ranging from 1 m<sup>2</sup> to 1000 m<sup>2</sup>. Given its extensive temporal and geographic  
137 coverage, this dataset is well-suited for interpolating biodiversity change. We modelled plot-  
138 level alpha diversity (species richness) of vascular plants as a function of plot size, spatial  
139 coordinates (latitude, longitude, and elevation), sampling year, and habitat type (forest,  
140 grassland, scrub, or wetland). To validate our interpolation approach, we tested its ability to  
141 predict temporal species richness changes using 22,852 independent resurvey time series from  
142 ReSurveyEurope within the same period. Specifically, we trained the model on a single  
143 randomly selected observation from each time series and evaluated its predictions against  
144 observed species richness changes in ReSurveyEurope. Our model successfully predicted the  
145 direction of species richness changes and explained 41% of the variability in those changes (see  
146 ‘Materials and Methods: Model Validation’). Having established the predictive power of our  
147 approach, we then applied it to temporally interpolate species richness dynamics across all  
148 vegetation plots sampled from 1960 to 2020, covering the last six decades across Europe.



149 **Figure 1:** Workflow for spatiotemporal interpolation of plant species richness ( $S$ ) and change in  
 150 species richness ( $\Delta S$ ) in European vegetation plots. Species richness ( $S$ ) from 698,692 static  
 151 vegetation plots (independent plot observations from different sites that are not paired in time)  
 152 sampled between 1945 to 2023 from the European Vegetation Archive (EVA) (Chytrý *et al.*  
 153 2016) and ReSurveyEurope (Knollová *et al.* 2024) is interpolated using machine learning as a  
 154 function of area, time, space, habitat type and their interactions aiming to maximize prediction  
 155 accuracy within the temporal dimension of the space-time cube (panel a). Interpolated values are  
 156 then used to estimate temporal changes in species richness (panel b). Colour coding of the dots in  
 157 panel a) represents species richness recorded in 10,000 randomly selected plots from the EVA  
 158 database for visualization.

## 159 2. Materials and Methods

### 160 2.1 Vegetation plot data

161 Our initial data set contained 1,679,403 vegetation plot observations available in the European  
 162 Vegetation archive (EVA) (Chytrý *et al.* 2016) and ReSurveyEurope (Knollová *et al.* 2024)

163 (project n. 222; version 2024-02-06: <https://doi.org/10.58060/jeht-nr04>). We restricted the  
164 analysis to plots with complete information on geographical location, habitat type, plot size, and  
165 sampling year, applying specific filters based on each of these variables. We included only plots  
166 with coordinate uncertainty below 1 km and focused exclusively on habitats classified as forest,  
167 grassland, scrub, wetland following the EUNIS habitat classification system (Chytrý *et al.* 2020).  
168 Additionally, we only included plots within defined size ranges (1-100 m<sup>2</sup> for non-forest habitats,  
169 100-1000 m<sup>2</sup> for forests) and sampled between 1945 and 2023. Further details on data cleaning  
170 and preparation are listed in Appendix S1. The application of these filters yielded a subset of  
171 675,840 vegetation plot observations in EVA and 73,886 observations across 22,852 resurvey  
172 plots in ReSurveyEurope (Fig. S1), which we used for all subsequent analyses. Both datasets  
173 were used for model training and interpolation. The ReSurveyEurope dataset was also used to  
174 test whether our approach could predict species richness dynamics observed in time series data  
175 (see ‘Model Validation’).

## 176 **2.2 Model training**

177 We used Random Forests (Breiman 2001) and Extreme Gradient Boosting (Chen & Guestrin  
178 2016) to model plot-level vascular plant species richness dependence on space (= elevation,  
179 latitude, and longitude) and time (= sampling year) while accounting for the effect of plot size  
180 and habitat type. We applied these algorithms because they are better suited to modelling  
181 complex interactions between predictors and their non-linear effects compared to generalized  
182 linear models and related parametric methods, which is a desirable property when the aim is to  
183 maximize accuracy of cross-scale predictions of biodiversity metrics (species richness or  
184 occupancy) and model grain-dependent interactions between time and spatial scales (Keil &  
185 Chase 2022, 2019; Leroy *et al.* 2024).

186 Our approach is based on *static* biodiversity data (in our case, vegetation plots surveyed only  
187 once) for spatiotemporal interpolation (Keil & Chase 2022). We trained the final model used in  
188 the interpolation analyses presented in the results of this work on a total of 698,692 vegetation  
189 plots, comprising 675,840 plots from EVA and 22,852 plots from ReSurveyEurope. Because  
190 plots from ReSurveyEurope have multiple observations, ranging from 2 to 46 (mean = 3.2; SD =  
191 3.5), we randomly selected one observation from each plot. The remaining 51,034 plot  
192 observations from ReSurveyEurope were excluded from the final model fit but were later used  
193 for model evaluation as test data (see the ‘Model Validation’ section).

194 Modelling was fully conducted in R (version 4.4.2) (R Core Team 2024) with the *tidymodels*  
195 (Kuhn & Wickham 2020) package collection and included the main steps described below.

- 196 - *Training/Test set splitting.* We randomly split the dataset into training (80% of  
197 observations) and testing (20% of observations) datasets. We stratified the split by the  
198 response variable (= species richness) to balance its distribution in both data sets.
- 199 - *Model specification.* We fitted models using vegetation plots as observation units, with  
200 the following formula:  $S \sim x + y + elevation + plot\ size + year + habitat\ type$ ; where  $S$   
201 represents vascular plant species richness;  $x$  and  $y$  are the coordinates (in meters) of  
202 easting and northing, respectively; *elevation* corresponds to elevation above the sea level  
203 (in meters); *plot size* is the area of the plot (in square meters); *year* is the year of  
204 sampling; and *habitat type* is a categorical variable describing the general habitat  
205 classification ('forest', 'grassland', 'scrub', or 'wetland'). We used the ‘ranger’ (Wright &  
206 Ziegler 2017) and ‘xgboost’ (Chen *et al.* 2024) engines available in the *parsnip* R  
207 package (Kuhn & Vaughan 2024) for Random Forests and Extreme Gradient Boosting  
208 algorithms, respectively.

209 - *Hyperparameter tuning.* We used a 10-fold random cross validation on the training data  
210 to perform hyperparameter tuning without repetition. We selected the best combinations  
211 of hyperparameters based on the lowest root mean square error (RMSE). For the Random  
212 Forests, we set the number of trees to 1000 and used a regular grid of 25 combinations of  
213 other hyperparameters, setting the minimum number of data points in a node for further  
214 splitting (= ‘node size’) to 2, 5, 10, 15, and 20, and the number of randomly sampled  
215 predictors (= ‘mtry’) from 2 to 6. For XGBoost, we tuned all possible hyperparameters  
216 (except for the number of trees, which was set to 1000) using default tuning parameters  
217 available in the *dials* R package (Kuhn & Frick 2024). We reduced the grid search for  
218 XGBoost by fitting 50 combinations of hyperparameters using a space filling design with  
219 latin hypercube grids with the ‘grid\_space\_filling’ function of the *dials* package. We used  
220 hyperparameter settings obtained from the tuning results of these Random Forests (node  
221 size = 5 and mtry = 3; see Fig. S4) as default hyperparameters in the final model fit and  
222 additional analyses.

223 - *Model evaluation.* We evaluated the models using a 10-fold cross-validation (repeated 3  
224 times) on the training data and on a separate testing dataset. The Random Forests  
225 algorithm (RMSE = 7.0,  $R^2 = 0.69$ ) performed better than the XGBoost algorithm (RMSE  
226 = 8.1,  $R^2 = 0.58$ ; Table S1). Therefore, in all subsequent analyses, we exclusively applied  
227 Random Forests. Finally, we validated that the distribution of model residuals did not  
228 exhibit geographical clusters by plotting the distribution of plot-level residuals calculated  
229 from the testing data (observed minus predicted species richness), averaged at a 50 km  
230 resolution (Fig. S5).

231 We also estimated the proportion of prediction variability explained by interactions between each

232 pair of predictors as well as the proportion of joint effect variability of pairwise interactions by  
233 calculating  $H^2$  statistics (Friedman & Popescu 2008) with the ‘hstats’ function from the *hstats* R  
234 package (Mayer 2024) (Fig. S6). We utilized the ‘partial\_dep’ function from the same package to  
235 visualize partial dependence plots (Fig. S7).

### 236 **2.3 Model validation**

237 To assess the reliability of our approach in estimating species richness dynamics, we trained  
238 separate Random Forests models on three static datasets: *A*) ReSurveyEurope, *B*) EVA, and *C*) a  
239 combination of both. To make the data in ReSurveyEurope ‘static’ (i.e., select one single plot  
240 observation at each vegetation plot site) for datasets *A* and *C*, we randomly selected one  
241 observation from each of the 22,852 resurvey plots. We split each of the three datasets, using  
242 80% of the data to train the models. We then evaluated their model performance separately based  
243 on the following observations from the three independent testing datasets:

- 244 1) *Species richness of the testing data*. Here, formal model evaluation was performed on the  
245 20% of data not used for model training during the data split.
- 246 2) *Species richness of data from ReSurveyEurope*. This included all plots from  
247 ReSurveyEurope that were not used for model training, i.e. the remaining 51,034  
248 independent plots neither used in training, nor in testing.
- 249 3) *Species richness change in ReSurveyEurope*. This was assessed using the log-response  
250 ratio (lnRR) of species richness between the initial and final plots within each resurvey  
251 time series. A positive correlation indicates that changes in species richness obtained  
252 from model predictions can capture observed changes in species richness.

253 We repeated the model training procedure 100 times for dataset *A*), each with a new random

254 selection of training and testing data from each time series. The model evaluation metrics  
255 showed that predictions were robust to random selection of plot combinations within the time  
256 series when tested using the criteria outlined in points 1, 2, and 3 (see Table S2).

257 Overall, our test demonstrated the feasibility of predicting species richness dynamics using  
258 interpolations from static data: when interpolating over ReSurveyEurope data, predicted and  
259 observed changes were positively correlated ( $R^2 = 0.41$ ; Pearson correlation = 0.64) (Fig. S8;  
260 Table S2). Predictions overall captured the observed direction of change, but they tended to  
261 slightly underestimate the observed magnitude of change, resulting in more conservative  
262 estimates (Fig. S9). However, models struggled to accurately predict species richness changes in  
263 new, spatially independent data, i.e. when EVA-only trained models were tested in  
264 ReSurveyEurope ( $R^2 = 0.06$ ; correlation = 0.23). This was likely due to an uneven spatial  
265 distribution of ReSurveyEurope plots relative to EVA plots, an overall higher error of predicting  
266 richness over two time periods for lnRR calculation, and different temporal distribution of EVA  
267 plots located closely to ReSurveyEurope. Finally, we found no significant differences in model  
268 validation results when comparing permanent and quasi-permanent ReSurveyEurope plots (Fig.  
269 S10), thus our approach is potentially robust against biases related to plot relocation.

270 In sum, our approach can explain up to 41% of the variability in species richness change over  
271 relatively long temporal spans (from 1945 to 2023). The evaluation of the model trained  
272 exclusively on EVA and tested on ReSurveyEurope data suggests that the results should not be  
273 geographically extrapolated beyond plot-level predictions. For these reasons, we used the  
274 interpolated spatiotemporal model to predict solely along the temporal dimension (i.e., we did  
275 not project the models outside the spatial scope of our data) and restricted the predictions of  
276 species richness dynamics exclusively to the plots utilized in the main model, combining data

277 from both EVA and ReSurveyEurope (see ‘Model training’ section).

## 278 **2.4 Interpolation of species richness change**

279 We used our model, trained on EVA and ReSurveyEurope data (see the ‘Model Training’  
280 section), to predict species richness for each year from 1960 to 2020. Predictions were made for  
281 the 660,748 plots included in the analysis and sampled during this period, while keeping other  
282 predictors fixed. To account for differences in plot size, we used the median plot size for each  
283 habitat type (forests: 300 m<sup>2</sup>, grasslands: 20 m<sup>2</sup>, scrub: 64 m<sup>2</sup>, wetlands: 50 m<sup>2</sup>) in our species  
284 richness predictions. To explore changes in species richness across the entire study period (1960-  
285 2020), we calculated the percentage change in interpolated species richness between 1960 and  
286 2020 for each plot, as follows:  $S_{change} = \frac{100*(S_{2020}-S_{1960})}{S_{1960}}$ . Similarly, we also calculated 21-year  
287 changes observed in 1980, 2000 and 2020, relative to that in the year 1960, 1980 and 2000,  
288 respectively.

289 We also examined temporal trends in mean species richness across all plots within each habitat  
290 type and across plots located in seven European biogeographical regions. For each year, we  
291 calculated the estimated mean species richness across all plots per habitat type or biogeographic  
292 region, respectively, and used it as the response variable in relation to year in a linear regression,  
293 effectively estimating the mean change in number of species per year. Biogeographical regions  
294 were sourced from the data of the European Environmental Agency (European Environment  
295 Agency 2016). We merged the arctic, boreal, and Scandinavian alpine regions into a single  
296 biogeographical unit, to distinguish these regions from the other alpine regions with nemoral-  
297 continental (e.g., the Alps, Carpathians, Pyrenees) and nemoral-submediterranean (e.g., Dinaric  
298 Alps, Rhodopes) vegetation (Preislerová *et al.* 2024).

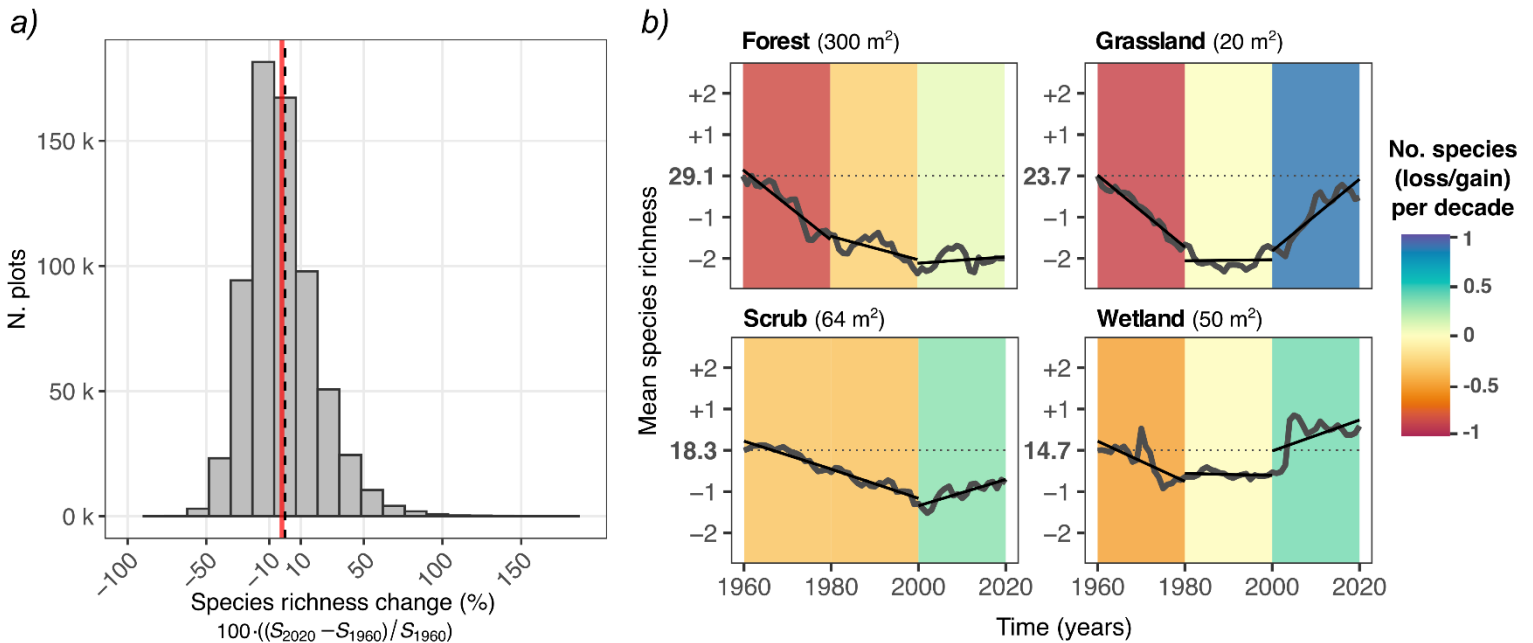
299 To visualize the geographic distribution of species richness change across the European  
300 continent, we aggregated plot-level percentages of species richness changes into 50 km × 50 km  
301 grids by averaging the predicted values of all plots in each raster cell. We plotted multiple maps  
302 for different time periods (1960–1980, 1980–2000, 2000–2020, and 1960–2020) and habitat  
303 types. Furthermore, to account for different temporal coverage of some cells (Fig. S2-S3), we  
304 calculated and mapped species richness change for each time period, including only plots  
305 sampled within each respective period to restrict the interpolations over shorter temporal gaps  
306 (Fig. S11). Similarly, we evaluated different metrics of species richness change, namely, log-  
307 response ratios (Fig. S12), the raw number of species lost or gained (Fig. S13), and linear slope  
308 estimates (Fig. S14) over the three periods (1960–1980, 1980–2000, and 2000–2020) separately,  
309 and across the entire focal period (1960–2020). Linear slope estimates were obtained by fitting  
310 linear regressions of predicted species richness against year for each plot, estimating the average  
311 number of species gained or lost per year over the assessed period. All these metrics quantifying  
312 diversity change exhibited overall consistent patterns with one another.

### 313 **3. Results and Discussion**

#### 314 **3.1 Balanced diversity changes, but shifting dynamics: early losses, late gains**

315 We estimated close to zero mean net change in species richness (-2%) between 1960 and 2020  
316 when averaged across all plots and habitat types (**Figure 2a**). This finding is similar to results of  
317 previous large-scale analyses of alpha diversity change, which show low net richness change  
318 across multiple time series (Bernhardt-Römermann *et al.* 2015; Blowes *et al.* 2019; Dornelas *et*  
319 *al.* 2014; Jandt *et al.* 2022; Vellend *et al.* 2013). Although the overall species loss in our analysis  
320 was minor, this average trend hides a substantial proportion of plots exhibiting large changes  
321 over the past six decades: 15% of plots showed a steep decline, with losses of more than 20% of

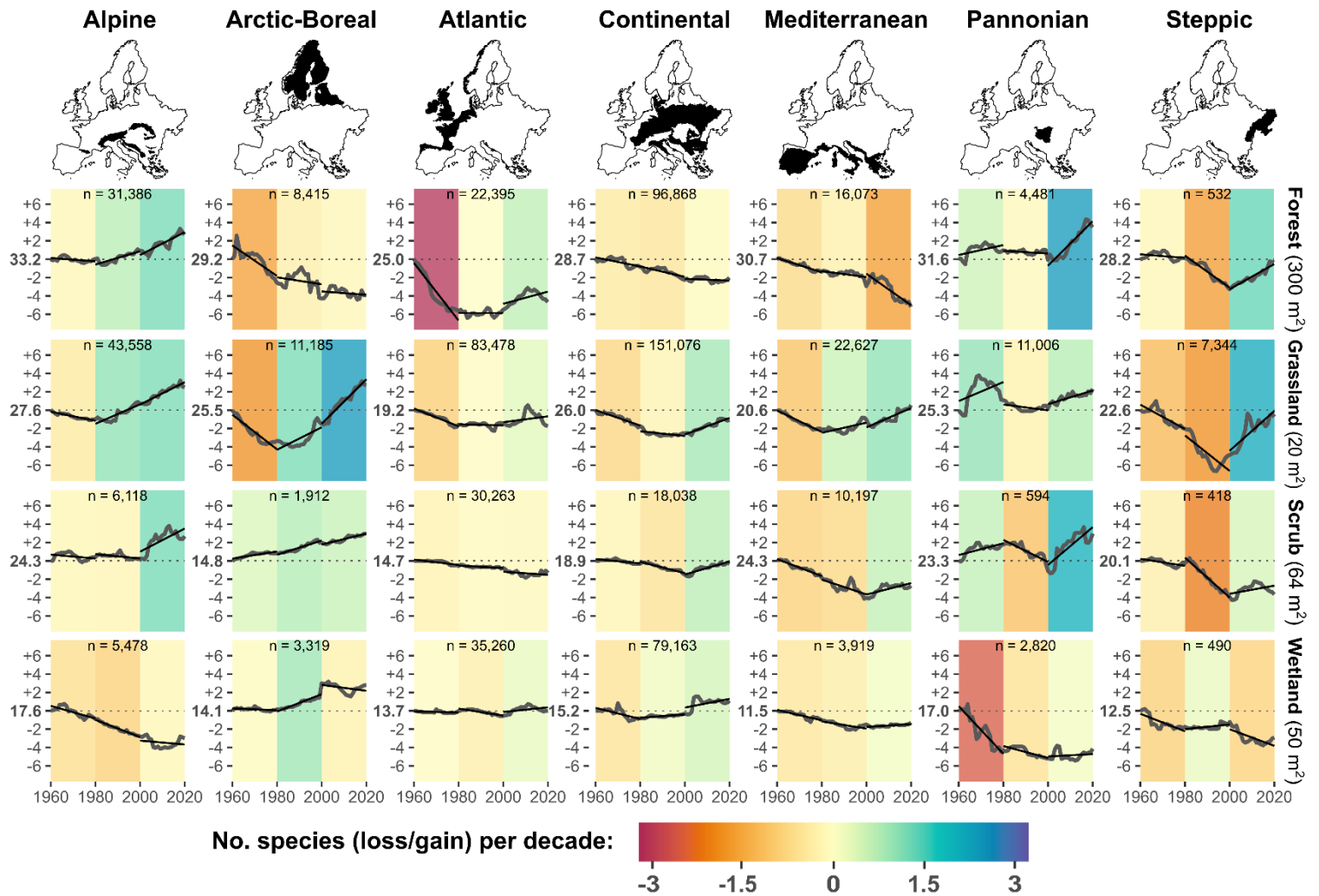
322 their initial species richness, while 19% of plots showed the opposite trend, with species gains of  
 323 more than 20%.



324 **Figure 2:** Summary of plant species richness changes over 61 years (1960–2020). Panel *a*)  
 325 shows the distribution of proportional change in interpolated plant species richness for the year  
 326 2020 compared to 1960 across 660,748 European vegetation plots sampled over that period.  
 327 Dashed vertical line corresponds to 0% change; red solid line to the mean (= -1.9%). Panel *b*)  
 328 shows temporal trends in average species richness (mean values across plots per year) for each  
 329 habitat (dark grey lines). Linear regressions (black lines) and their slopes (coloured backgrounds)  
 330 are fitted to species richness for three time periods: 1960–1980, 1980–2000, and 2000–2020. The  
 331 y-axis scale is standardized to the baseline mean species richness estimated for the year 1960. To  
 332 standardize differences in plot size, species richness was predicted using a fixed plot size equal  
 333 to the median plot size for each habitat (noted at the top of each panel).

334 We identified shifting dynamics over time characterized by a prevailing decline in species  
 335 richness from 1960 to 1980 (continuing up to the 2000s in forests and scrubs), followed by gains  
 336 in species richness from 2000 to 2020 across all habitat types (**Figure 2b**) and in most  
 337 biogeographic regions (**Figure 3**). While our approach cannot establish a causal link between  
 338 species richness changes and potential underlying drivers, the greater losses detected during  
 339 earlier decades align with well-documented factors contributing to European biodiversity

340 decline. These factors include agricultural intensification and eutrophication driven by nitrogen  
341 (N) and phosphorus (P) enrichment, along with acid deposition, all of which began increasing in  
342 the early 20th century and peaked in the latter half of the century (Araújo *et al.* 2008; Fuchs *et al.*  
343 2015; Schöpp *et al.* 2003; de Vries *et al.* 2024). Each of these drivers has likely impacted  
344 different habitats to a different extent, such as acidic deposition in forests (Hédli 2004), and soil  
345 drainage and nitrogen deposition favouring encroachment by generalist species in wetlands  
346 (Sperle & Bruelheide 2021) and grasslands (Stevens *et al.* 2010). As recently shown for the flora  
347 of the Czech Republic (Klinkovská *et al.* 2024), industrialization and land-use intensification  
348 during the 1960-1980s has generally advantaged species adapted to anthropogenic disturbances  
349 and high nutrient availability. Especially high rates of eutrophication in European countries  
350 during this period likely contributed to species richness declines, by promoting the dominance of  
351 a few species favoured by high nitrogen availability (Staude *et al.* 2020; Stevens *et al.* 2010).  
352 These declines were lessened over time when species numbers gradually reduced as  
353 compositions shifted to more nitrophilous vegetation (Bobbink *et al.* 2010), with possible species  
354 richness recovery following reduced N input (Storkey *et al.* 2015).



355 **Figure 3:** Trends of species richness change over 61 years (1960-2020) in seven European  
 356 biogeographic regions. Each panel displays the estimated trend (dark grey curves) of the mean  
 357 interpolated species richness (y-axis) across all plots within a given biogeographic region and  
 358 habitat type over time (x-axis). The number of plots (n) is indicated at the top of each panel.  
 359 Linear regressions (black lines) and their slopes (coloured backgrounds) are fitted to species  
 360 richness for three time periods: 1960–1980, 1980–2000, and 2000–2020. The y-axis scale is  
 361 standardized to the baseline mean species richness estimated for the year 1960. Species richness  
 362 was predicted using a fixed plot size equal to the median plot size for each habitat (noted at the  
 363 right for each habitat).

364 Subsequently, the increased occupancy of warm-adapted and non-native species (Klinkovská *et*  
 365 *al.* 2024), along with overall range shifts of species tracking their thermal niches in response to  
 366 climate change (Rumpf *et al.* 2018), may have contributed to local species recruitment in recent  
 367 decades (2000-2020), resulting in a species richness increase. This trend was particularly

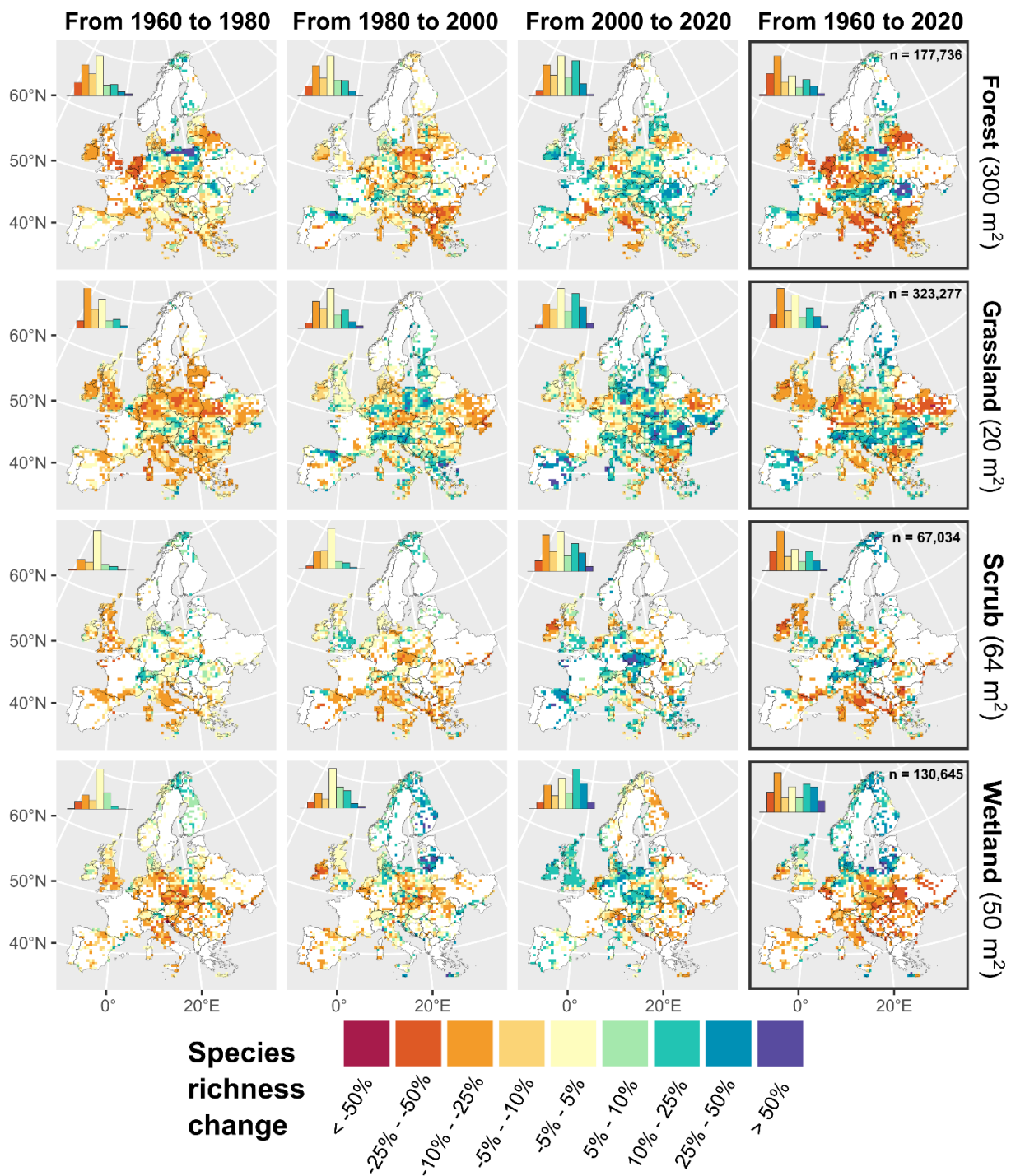
368 noticeable at higher latitudes (e.g., in open habitats of the boreal region) and in mountainous  
369 areas (**Figure 3** and **Figure 4**), and corroborates previous studies focusing on these ecosystems  
370 and regions (Steinbauer *et al.* 2018; Thuiller *et al.* 2005). Furthermore, species richness gains  
371 observed since the 2000s could partially reflect the Europe-wide abatement of airborne  
372 anthropogenic N and sulphur (S) deposition from the 1990s onwards (Sutton *et al.* 2011; de  
373 Vries *et al.* 2024), as well as more recent improvements in nature conservation and restoration  
374 policies supported by the European Union [e.g., the 1992 Habitats Directive (European Union  
375 1992)]. Preferential sampling could partly explain the observed positive trends in species  
376 richness in some regions over the last decades. However, to our knowledge, this bias applies only  
377 to those regions where older vegetation surveys, focusing on phytosociological classification  
378 (sometimes omitting certain species from the plots, leading to an underestimation of richness),  
379 shifted toward sampling of better-preserved vegetation over more recent years (e.g., due to  
380 monitoring over protected areas). Yet, older surveys often targeted floristically richer sites, while  
381 recent efforts more often include degraded sites too, potentially balancing these trends.

### 382 **3.2 Habitat- and region-specific diversity change**

383 We found highly context-dependent trajectories of species richness change (**Figure 3** and **Figure**  
384 **4**), consistent with studies challenging the notion of unidirectional biodiversity change (Dornelas  
385 *et al.* 2023; Johnson *et al.* 2024; Pilotto *et al.* 2020) and supporting the idea that biodiversity  
386 change depends on habitat type (Klinkovská *et al.* 2025), geographic location  
387 (Bernhardt-Römermann *et al.* 2015; Blowes *et al.* 2019), and, most crucially, time period  
388 considered. Although significant geographic heterogeneity in interpolated species richness trends  
389 was observed across Europe, a few distinct geographic patterns emerged. Overall, colder regions,  
390 namely the alpine and the arctic-boreal zones, showed increases in species richness, although

391 localized declines were observed in wetlands and forests within these regions; conversely, other  
392 regions displayed either stable trends or overall losses.

393 When comparing 2020 to 1960, forest habitats showed the highest proportion of plots with  
394 substantial declines of species richness compared to other habitats, with 25% of plots estimated  
395 to have lost  $\leq 20\%$  of species, and a mean change of  $-6\%$ . Large declines in forests are  
396 interpretable as results of alteration of management practices (i.e., cessation of coppicing and  
397 forest grazing coupled with increased canopy density), resulting in a shift towards species-poorer  
398 communities representative of denser, moister, and nutrient-richer conditions (i.e., mesification)  
399 (Hédli *et al.* 2010; Lelli *et al.* 2021). Our findings partially contrast with the synthesis by  
400 Bernhardt-Römermann *et al.* (2015) on resurvey studies of forest vegetation in Europe, which  
401 reported more balanced trends for this habitat type. However, their study covered fewer old sites,  
402 potentially reducing their chance to detect losses that occurred in the 1960s or earlier  
403 (particularly in the Atlantic region), and focused on temperate forests only. Indeed, we identified  
404 constant declines of species richness in boreal and Mediterranean forests (**Figure 3**).  
405 Interestingly, forests in the Alpine region displayed an opposite, positive trend. These variations  
406 across biogeographic regions reflect the notion that local and regional drivers specific to forest  
407 habitats – such as changes in large ungulate densities, management practices, and their  
408 interactions with nitrogen deposition and global warming – create context-dependent impacts on  
409 plant species richness dynamics of forest vegetation (Bernhardt-Römermann *et al.* 2015; Perring  
410 *et al.* 2018; Staude *et al.* 2020).



411 **Figure 4:** Geographic patterns of plant species richness change in Europe. The maps show the  
 412 mean percentage change in plot-level species richness between two time points, aggregated  
 413 within 50 km × 50 km grid cells. Only grid cells containing at least five plots sampled between  
 414 1960 and 2020 are shown. Histograms (upper left of each panel) illustrate the distribution of  
 415 percentage change classes across all plots. The number of plots (n) for each habitat is shown in  
 416 the panels on the right that estimate richness changes from 1960 to 2020. Species richness was  
 417 predicted using a fixed plot size equal to the median plot size for each habitat (noted on the right  
 418 for each habitat).

419 Grasslands displayed more balanced trends, with a net species richness change close to zero  
420 (mean: -1.5%) over the whole study period. The high heterogeneity of grassland diversity trends  
421 across Europe (**Figure 4**) could reflect, among many other drivers, highly localized management  
422 practices, ranging from strong intensification to complete abandonment, creating a patchy  
423 mosaic of biodiversity trends across European grasslands (Shipley *et al.* 2024). Conversely,  
424 wetlands had the most polarized results, with large fractions of plots showing high gains and  
425 losses ( $\geq 20\%$ ) in 25% and 18% of the plots, respectively, resulting in a slightly positive average  
426 change (mean: +4%) across the whole study period. Compared to other habitats, wetlands also  
427 displayed a more distinct geographical gradient: plots with increasing richness or no change were  
428 primarily located at higher latitudes (above  $55^\circ$  N). Given the substantial pressures affecting  
429 most European wetland ecosystems (Verhoeven 2014), we did not expect large gains in  
430 wetlands. This sharp latitudinal pattern may reflect changes in local hydrological regimes (e.g.,  
431 soil drainage) that promote the encroachment of generalist vascular plant species resulting in  
432 higher species richness, at the expense of typical moss species (not included in our analysis)  
433 found in northern European mires (Kolari *et al.* 2021; Pedrotti *et al.* 2014). The higher  
434 magnitude of change in wetlands also likely reflects their generally lower baseline vascular  
435 species richness (see Fig. S7), where the addition of a few species can strongly affect gains in  
436 species richness. Nonetheless, most wetlands at lower latitudes, especially in Central Europe  
437 (**Figure 4**), experienced large losses in species richness. This find accords with previous studies  
438 of wetlands in central and southern European lowlands, which have documented climate change  
439 toward warmer conditions, combined with drastic increases in human water extraction from  
440 natural systems, as key drivers of wetland specialist losses (Navrátilová *et al.* 2022; Sperle &  
441 Bruelheide 2021).

#### 442 **4. Advances, limitations, and implications for addressing biodiversity change**

443 With this study, we provide the first continental-scale analysis of local biodiversity change over  
444 continuous time and space, unlocking an unprecedented amount of vegetation-plot data collected  
445 over more than six decades. Compared to previous large-scale analyses of time series data  
446 (Bernhardt-Römermann *et al.* 2015; Blowes *et al.* 2019; Dornelas *et al.* 2014; Jandt *et al.* 2022;  
447 Klinkovská *et al.* 2025; Pilotto *et al.* 2020; Vellend *et al.* 2013), our approach enabled us to i)  
448 unravel these trends across a broad geographic extent and different habitat types and ii) compare  
449 them to common baselines from the same time period. This was previously difficult to achieve at  
450 the continental scale due to data limitations and because past methods rarely leveraged static data  
451 to inform analyses of biodiversity dynamics (Jandt *et al.* 2011). Our new method addresses the  
452 latter and can potentially be applied to other taxonomic groups and spatial grains (Keil & Chase  
453 2022; Leroy *et al.* 2024) to robustly estimate biodiversity change even in the absence of  
454 dedicated time series data. Additionally, our method can be applied to individual species  
455 occurrences, offering potential for studies mapping single-species dynamics and composition  
456 changes, although this may involve considerable computational costs. Our work is intended to  
457 complement, rather than replace, the efforts of field ecologists to resurvey vegetation and collect  
458 new data, which are the fundamental source for assessing spatial and temporal patterns of  
459 biodiversity. Indeed, geographically and temporally representative long-term monitoring of  
460 habitats across Europe is essential for effectively assessing, preserving, and restoring  
461 biodiversity (Moersberger *et al.* 2024). Such monitoring data are crucial not only for  
462 understanding biodiversity change but also for enhancing the validation of our method from non-  
463 systematic data sources like those employed here.

464 While our approach provides a robust assessment of regional-scale biodiversity trends (i.e., the

465 average local trend in a larger region), as indicated by the results of our model validation (see  
466 Fig. S8), it is likely weaker at making precise predictions at individual sites, as indicated by the  
467 59% of variance in species richness that was not explained by our predictions. In addition,  
468 although habitat changes (e.g., a transition from grassland to scrub) can be integrated into model  
469 predictions, our approach does not account for local land-use changes or intensification, such as  
470 the destruction of surveyed plant communities due to deforestation, urbanization, or agricultural  
471 conversion. In other words, our method is conservative in estimating local species richness  
472 change, assuming the preservation of each community type within the time window assessed.  
473 Furthermore, we caution that this method may yield unreliable estimates in regions lacking  
474 sufficient temporal coverage of geographically close observations in areas that are poorly  
475 sampled over time (but see Fig. S5).

476 Species richness dynamics revealed by our study have several key implications for biodiversity  
477 assessment and conservation planning in Europe. Our results suggest that vegetation plots  
478 experiencing local losses in species richness could also experience gains in the future. Yet, in  
479 many cases, a local increase in species richness should not necessarily be interpreted as an  
480 improvement in conservation status but could instead indicate habitat quality deterioration  
481 (namely, losses in habitat specialists in favour of generalist or non-native species colonizing  
482 plant communities and increasing local alpha diversity) (Jandt *et al.* 2022; Klinkovská *et al.*  
483 2025). Further investigation of long-term plant diversity trends at broader scales and beyond  
484 alpha diversity (e.g., habitat specialist occupancy) is needed to confirm whether the recent rise in  
485 local species richness across habitats results from biotic homogenization by generalists and alien  
486 species at the expense of specialists. Given the large geographic heterogeneity of diversity trends  
487 that we uncovered, we nonetheless emphasize the importance of recognizing regional variations

488 when implementing conservation and restoration actions. This means tailoring the  
489 implementation of joint EU policies, such as the Agri-Environment Schemes (European  
490 Commission 2017), the Common Agricultural Policy (CAP) (European Commission 2012), and  
491 the Nature Restoration Law(European Commission 2023), to prioritize local and habitat-specific  
492 conservation and restoration needs.

### 493 **Acknowledgements**

494 We thank colleagues who sampled vegetation plots in the field or digitized them into the  
495 databases used in this work. G.M, P.K, and A.T.C. were supported by the Czech Science  
496 Foundation (project no. 24-14299L) and the Austrian Science Foundation FWF (project no. I  
497 6578) as part of the GRACE project. P.K. was funded by the European Union (ERC, BEAST,  
498 101044740). Views and opinions expressed are however those of the author(s) only and do not  
499 necessarily reflect those of the European Union or the European Research Council Executive  
500 Agency. Neither the European Union nor the granting authority can be held responsible for them.  
501 M.C., J.Di., and M.V. were supported by the Czech Science Foundation (project no. 25-15235S).  
502 U.J. and H.B. acknowledge funding from Biodiversa+ in the context of the MOTIVATE project  
503 under the 2022-2023 BiodivMon joint call, co-funded by the European Commission (GA No.  
504 101052342) and the German Research Foundation (DFG) project number 532411638. I.B. and  
505 I.S. were supported by the Basque Government (IT487-22). I.S. was also supported by the  
506 University of the Basque Country predoctoral grant (PIF21/255). B.J.A. was supported by the  
507 EU, the Principality of Asturias and the SEKUENS Agency through the GRUPIN grants. J.C.S  
508 was supported by Center for Ecological Dynamics in a Novel Biosphere (ECONOVO), funded  
509 by Danish National Research Foundation (grant DNRF173).

## 510 **References**

- 511 Araújo, M.B., Nogués-Bravo, D., Reginster, I., Rounsevell, M. & Whittaker, R.J. (2008).  
512 Exposure of European biodiversity to changes in human-induced pressures. *Environ Sci*  
513 *Policy*, 11, 38–45.
- 514 Bernhardt-Römermann, M., Baeten, L., Craven, D., De Frenne, P., Hédli, R., Lenoir, J., *et al.*  
515 (2015). Drivers of temporal changes in temperate forest plant diversity vary across spatial  
516 scales. *Glob Chang Biol*, 21, 3726–3737.
- 517 Blowes, S.A., Supp, S.R., Antão, L.H., Bates, A., Bruelheide, H., Chase, J.M., *et al.* (2019). The  
518 geography of biodiversity change in marine and terrestrial assemblages. *Science (1979)*,  
519 366, 339–345.
- 520 Bobbink, R., Hicks, K., Galloway, J., Spranger, T., Alkemade, R., Ashmore, M., *et al.* (2010).  
521 Global assessment of nitrogen deposition effects on terrestrial plant diversity: a synthesis.  
522 *Ecological Applications*, 20, 30–59.
- 523 Boch, S., Kuchler, H., Kuchler, M., Bedolla, A., Ecker, K.T., Graf, U.H., *et al.* (2022). Observer-  
524 driven pseudoturnover in vegetation monitoring is context-dependent but does not affect  
525 ecological inference. *Appl Veg Sci*, 25, e12669.
- 526 Breiman, L. (2001). Random forests. *Mach Learn*, 45, 5–32.
- 527 Chen, T. & Guestrin, C. (2016). XGBoost: A scalable tree boosting system. *Proceedings of the*  
528 *ACM SIGKDD International Conference on Knowledge Discovery and Data Mining*, 13-  
529 17-August-2016, 785–794.
- 530 Chen, T., He, T., Benesty, M., Khotilovich, V., Tang, Y., Cho, H., *et al.* (2024). *xgboost:*  
531 *Extreme Gradient Boosting. R package version 1.7.8.1.* Available at: [https://CRAN.R-](https://CRAN.R-project.org/package=xgboost)  
532 [project.org/package=xgboost](https://CRAN.R-project.org/package=xgboost). Last accessed 23 November 2024.
- 533 Chytrý, M., Hennekens, S.M., Jiménez-Alfaro, B., Knollová, I., Dengler, J., Jansen, F., *et al.*  
534 (2016). European Vegetation Archive (EVA): an integrated database of European  
535 vegetation plots. *Appl Veg Sci*, 19, 173–180.
- 536 Chytrý, M., Tichý, L., Hennekens, S.M., Knollová, I., Janssen, J.A.M., Rodwell, J.S., *et al.*  
537 (2020). EUNIS Habitat Classification: Expert system, characteristic species combinations

538 and distribution maps of European habitats. *Appl Veg Sci*, 23, 648–675.

539 Dengler, J., Matthews, T.J., Steinbauer, M.J., Wolfrum, S., Boch, S., Chiarucci, A., *et al.* (2020).  
540 Species–area relationships in continuous vegetation: Evidence from Palaearctic grasslands.  
541 *J Biogeogr*, 47, 72–86.

542 Díaz, S., Settele, J., Brondízio, E.S., Ngo, H.T., Agard, J., Arneth, A., *et al.* (2019). Pervasive  
543 human-driven decline of life on Earth points to the need for transformative change. *Science*  
544 (1979), 366.

545 Dornelas, M., Chase, J.M., Gotelli, N.J., Magurran, A.E., McGill, B.J., Antão, L.H., *et al.*  
546 (2023). Looking back on biodiversity change: lessons for the road ahead. *Philosophical*  
547 *Transactions of the Royal Society B*, 378.

548 Dornelas, M., Gotelli, N.J., McGill, B., Shimadzu, H., Moyes, F., Sievers, C., *et al.* (2014).  
549 Assemblage time series reveal biodiversity change but not systematic loss. *Science (1979)*,  
550 344, 296–299.

551 Dornelas, M., Magurran, A.E., Buckland, S.T., Chao, A., Chazdon, R.L., Colwell, R.K., *et al.*  
552 (2013). Quantifying temporal change in biodiversity: challenges and opportunities.  
553 *Proceedings of the Royal Society B: Biological Sciences*, 280, 20121931.

554 Dullinger, S., Essl, F., Rabitsch, W., Erb, K.-H., Gingrich, S., Haberl, H., *et al.* (2013). Europe’s  
555 other debt crisis caused by the long legacy of future extinctions. *Proceedings of the*  
556 *National Academy of Sciences*, 110, 7342–7347.

557 European Commission. (2012). *The Common Agricultural Policy – A partnership between*  
558 *Europe and farmers*. Publications Office.

559 European Commission. (2017). *Agri-environment schemes – Impacts on the agricultural*  
560 *environment*. Publications Office.

561 European Commission. (2023). *Impact assessment study to support the development of legally*  
562 *binding EU nature restoration targets – Final report*. Publications Office of the European  
563 Union.

564 European Environment Agency. (2016). *Biogeographical regions in Europe*. Available at:  
565 <https://www.eea.europa.eu/en/analysis/maps-and-charts/biogeographical-regions-in-europe->

566           2?activeTab=8a280073-bf94-4717-b3e2-1374b57ca99d. Last accessed 24 November 2024.

567 European Union. (1992). Council Directive 92/43/EEC of 21 May 1992 on the Conservation of  
568 Natural Habitats and of Wild Fauna and Flora. *Official Journal of the European*  
569 *Communities*, L 206, 7–50.

570 Finderup Nielsen, T., Sand-Jensen, K. & Bruun, H.H. (2021). Drier, darker and more fertile: 140  
571 years of plant habitat change driven by land-use intensification. *Journal of Vegetation*  
572 *Science*, 32.

573 Friedman, J.H. & Popescu, B.E. (2008). Predictive learning via rule ensembles. *Ann Appl Stat*, 2.

574 Fuchs, R., Herold, M., Verburg, P.H., Clevers, J.G.P.W. & Eberle, J. (2015). Gross changes in  
575 reconstructions of historic land cover/use for Europe between 1900 and 2010. *Glob Chang*  
576 *Biol*, 21, 299–313.

577 Gonzalez, A., Cardinale, B.J., Allington, G.R.H., Byrnes, J., Endsley, K.A., Brown, D.G., *et al.*  
578 (2016). Estimating local biodiversity change: a critique of papers claiming no net loss of  
579 local diversity. *Ecology*, 97, 1949–1960.

580 Gray, C.L., Hill, S.L.L., Newbold, T., Hudson, L.N., Boirger, L., Contu, S., *et al.* (2016). Local  
581 biodiversity is higher inside than outside terrestrial protected areas worldwide. *Nature*  
582 *Communications 2016 7:1*, 7, 1–7.

583 Hédli, R. (2004). Vegetation of beech forests in the Rychlebské Mountains, Czech Republic, re-  
584 inspected after 60 years with assessment of environmental changes. *Plant Ecol*, 170, 243–  
585 265.

586 Hédli, R., Kopecký, M. & Komárek, J. (2010). Half a century of succession in a temperate  
587 oakwood: from species-rich community to mesic forest. *Divers Distrib*, 16, 267–276.

588 IPBES. (2019). Global Assessment Report on Biodiversity and Ecosystem Services of the  
589 Intergovernmental Science-Policy Platform on Biodiversity and Ecosystem Services.

590 Jandt, U., Bruelheide, H., Jansen, F., Bonn, A., Grescho, V., Klenke, R.A., *et al.* (2022). More  
591 losses than gains during one century of plant biodiversity change in Germany. *Nature 2022*  
592 *611:7936*, 611, 512–518.

593 Jandt, U., von Wehrden, H. & Bruelheide, H. (2011). Exploring large vegetation databases to

594 detect temporal trends in species occurrences. *Journal of Vegetation Science*, 22, 957–972.

595 Johnson, T.F., Beckerman, A.P., Childs, D.Z., Webb, T.J., Evans, K.L., Griffiths, C.A., *et al.*  
596 (2024). Revealing uncertainty in the status of biodiversity change. *Nature* 2024 628:8009,  
597 628, 788–794.

598 Keil, P. & Chase, J. (2022). Interpolation of temporal biodiversity change, loss, and gain across  
599 scales: a machine learning approach. *EcoEvoRxiv*.

600 Keil, P. & Chase, J.M. (2019). Global patterns and drivers of tree diversity integrated across a  
601 continuum of spatial grains. *Nature Ecology & Evolution* 2019 3:3, 3, 390–399.

602 Klinkovská, K., Glaser, M., Danihelka, J., Kaplan, Z., Knollová, I., Novotný, P., *et al.* (2024).  
603 Dynamics of the Czech flora over the last 60 years: Winners, losers and causes of changes.  
604 *Biol Conserv*, 292, 110502.

605 Klinkovská, K., Marta, |, Sperandii, G., Knollová, I., Danihelka, | Jiří, Hájek, M., *et al.* (2025).  
606 Half a Century of Temperate Non-Forest Vegetation Changes: No Net Loss in Species  
607 Richness, but Considerable Shifts in Taxonomic and Functional Composition. *Glob Chang*  
608 *Biol*, 31, e70030.

609 Knollová, I., Chytrý, M., Bruehlheide, H., Dullinger, S., Jandt, U., Bernhardt-Römermann, M., *et*  
610 *al.* (2024). ReSurveyEurope: A database of resurveyed vegetation plots in Europe. *Journal*  
611 *of Vegetation Science*, 35, e13235.

612 Kolari, T.H.M., Korpelainen, P., Kumpula, T. & Tahvanainen, T. (2021). Accelerated vegetation  
613 succession but no hydrological change in a boreal fen during 20 years of recent climate  
614 change. *Ecol Evol*, 11, 7602–7621.

615 Kuhn, M. & Frick, H. (2024). *dials: Tools for Creating Tuning Parameter Values*. *R package*  
616 *version 1.2.1*. Available at: <https://CRAN.R-project.org/package=dials>. Last accessed 23  
617 November 2024.

618 Kuhn, M. & Vaughan, D. (2024). *parsnip: A Common API to Modeling and Analysis Functions*.  
619 *R package version 1.2.1*. Available at: <https://CRAN.R-project.org/package=parsnip>. Last  
620 accessed 23 November 2024.

621 Kuhn, M. & Wickham, H. (2020). *Tidymodels: a collection of packages for modeling and*

622 *machine learning using tidyverse principles*. Available at: <https://www.tidymodels.org>. Last  
623 accessed 23 November 2024.

624 Legendre, P. (1993). Spatial autocorrelation: trouble or new paradigm? *Ecology*, 74, 1659–1673.

625 Lelli, C., Nascimbene, J., Alberti, D., Agostini, N., Zoccola, A., Piovesan, G., *et al.* (2021).  
626 Long-term changes in Italian mountain forests detected by resurvey of historical vegetation  
627 data. *Journal of Vegetation Science*, 32.

628 Leroy, F., Reif, J., Vermouzek, Z., Šťastný, K., Trávníčková, E., Bejček, V., *et al.* (2024).  
629 Decomposing biodiversity change to processes of extinction, colonization, and recurrence  
630 across scales. *Ecography*, 2024.

631 Mahecha, M.D., Gans, F., Brandt, G., Christiansen, R., Cornell, S.E., Fomferra, N., *et al.* (2020).  
632 Earth system data cubes unravel global multivariate dynamics. *Earth System Dynamics*, 11,  
633 201–234.

634 Mayer, M. (2024). *hstats: Interaction Statistics*. Available at: [https://CRAN.R-](https://CRAN.R-project.org/package=hstats)  
635 [project.org/package=hstats](https://CRAN.R-project.org/package=hstats). Last accessed 27 November 2024.

636 Moersberger, H., Valdez, J., Martin, J.G.C., Junker, J., Georgieva, I., Bauer, S., *et al.* (2024).  
637 Biodiversity monitoring in Europe: User and policy needs. *Conserv Lett*, 17.

638 Navrátilová, J., Navrátil, J. & Hájek, M. (2022). Medium-term changes of vegetation  
639 composition on fens of the rural landscape, tested using fixed permanent plots. *Folia*  
640 *Geobot*, 57, 151–166.

641 Pedrotti, E., Rydin, H., Ingmar, T., Hytteborn, H., Turunen, P. & Granath, G. (2014). Fine-scale  
642 dynamics and community stability in boreal peatlands: revisiting a fen and a bog in Sweden  
643 after 50 years. *Ecosphere*, 5, 1–24.

644 Perring, M.P., Bernhardt-Römermann, M., Baeten, L., Midolo, G., Blondeel, H., Depauw, L., *et*  
645 *al.* (2018). Global environmental change effects on plant community composition  
646 trajectories depend upon management legacies. *Glob Chang Biol*, 24, 1722–1740.

647 Pilotto, F., Kühn, I., Adrian, R., Alber, R., Alignier, A., Andrews, C., *et al.* (2020). Meta-  
648 analysis of multidecadal biodiversity trends in Europe. *Nature Communications* 2020 11:1,  
649 11, 1–11.

650 Preislerová, Z., Marcenò, C., Loidi, J., Bonari, G., Borovyk, D., Gavilán, R.G., *et al.* (2024).  
651 Structural, ecological and biogeographical attributes of European vegetation alliances. *Appl*  
652 *Veg Sci*, 27, e12766.

653 R Core Team. (2024). *R: A Language and Environment for Statistical Computing. version 4.3.1.*  
654 Available at: <https://www.R-project.org/>. Last accessed 23 November 2024.

655 Rumpf, S.B., Hülber, K., Klöner, G., Moser, D., Schütz, M., Wessely, J., *et al.* (2018). Range  
656 dynamics of mountain plants decrease with elevation. *Proc Natl Acad Sci U S A*, 115, 1848–  
657 1853.

658 Schöpp, W., Posch, M., Mylona, S. & Johansson, M. (2003). Long-term development of acid  
659 deposition (1880–2030) in sensitive freshwater regions in Europe. *Hydrol Earth Syst Sci*, 7,  
660 436–446.

661 Shipley, J.R., Frei, E.R., Bergamini, A., Boch, S., Schulz, T., Ginzler, C., *et al.* (2024).  
662 Agricultural practices and biodiversity: Conservation policies for semi-natural grasslands in  
663 Europe. *Current Biology*, 34, R753–R761.

664 Sperle, T. & Bruehlheide, H. (2021). Climate change aggravates bog species extinctions in the  
665 Black Forest (Germany). *Divers Distrib*, 27, 282–295.

666 Staude, I.R., Waller, D.M., Bernhardt-Römermann, M., Bjorkman, A.D., Brunet, J., De Frenne,  
667 P., *et al.* (2020). Replacements of small- by large-ranged species scale up to diversity loss in  
668 Europe’s temperate forest biome. *Nat Ecol Evol*, 4, 802–808.

669 Steinbauer, M.J., Grytnes, J.A., Jurasinski, G., Kulonen, A., Lenoir, J., Pauli, H., *et al.* (2018).  
670 Accelerated increase in plant species richness on mountain summits is linked to warming.  
671 *Nature* 2018 556:7700, 556, 231–234.

672 Stevens, C.J., Dupr, C., Dorland, E., Gaudnik, C., Gowing, D.J.G., Bleeker, A., *et al.* (2010).  
673 Nitrogen deposition threatens species richness of grasslands across Europe. *Environmental*  
674 *Pollution*, 158, 2940–2945.

675 Storch, D. (2016). The theory of the nested species–area relationship: geometric foundations of  
676 biodiversity scaling. *Journal of Vegetation Science*, 27, 880–891.

677 Storkey, J., Macdonald, A.J., Poulton, P.R., Scott, T., Köhler, I.H., Schnyder, H., *et al.* (2015).

678 Grassland biodiversity bounces back from long-term nitrogen addition. *Nature* 2015  
679 528:7582, 528, 401–404.

680 Sutton, M., Howard, C., Erismann, J., Billen, G., Bleeker, A., Grennfelt, P., *et al.* (2011). *The*  
681 *European Nitrogen Assessment*. Cambridge University Press.

682 Thuiller, W., Lavorel, S., Araújo, M.B., Sykes, M.T. & Prentice, I.C. (2005). Climate change  
683 threats to plant diversity in Europe. *Proceedings of the National Academy of Sciences*, 102,  
684 8245–8250.

685 Tobler, W.R. (1970). A Computer Movie Simulating Urban Growth in the Detroit Region. *Econ*  
686 *Geogr*, 46, 234.

687 Vellend, M., Baeten, L., Becker-Scarpitta, A., Boucher-Lalonde, V., McCune, J.L., Messier, J.,  
688 *et al.* (2017). Plant Biodiversity Change Across Scales During the Anthropocene. *Annu Rev*  
689 *Plant Biol*, 68, 563–586.

690 Vellend, M., Baeten, L., Myers-Smith, I.H., Elmendorf, S.C., Beauséjour, R., Brown, C.D., *et al.*  
691 (2013). Global meta-analysis reveals no net change in local-scale plant biodiversity over  
692 time. *Proceedings of the National Academy of Sciences*, 110, 19456–19459.

693 Verheyen, K., Bažány, M., Chečko, E., Chudomelová, M., Closset-Kopp, D., Czortek, P., *et al.*  
694 (2018). Observer and relocation errors matter in resurveys of historical vegetation plots.  
695 *Journal of Vegetation Science*, 29, 812–823.

696 Verhoeven, J.T.A. (2014). Wetlands in Europe: Perspectives for restoration of a lost paradise.  
697 *Ecol Eng*, 66, 6–9.

698 Vilà, M., Espinar, J.L., Hejda, M., Hulme, P.E., Jarošík, V., Maron, J.L., *et al.* (2011). Ecological  
699 impacts of invasive alien plants: a meta-analysis of their effects on species, communities  
700 and ecosystems. *Ecol Lett*, 14, 702–708.

701 de Vries, W., Posch, M., Simpson, D., de Leeuw, F.A.A.M., van Grinsven, H.J.M., Schulte-  
702 Uebbing, L.F., *et al.* (2024). Trends and geographic variation in adverse impacts of nitrogen  
703 use in Europe on human health, climate, and ecosystems: A review. *Earth Sci Rev*, 253,  
704 104789.

705 Wesche, K., Krause, B., Culmsee, H. & Leuschner, C. (2012). Fifty years of change in Central

706 European grassland vegetation: Large losses in species richness and animal-pollinated  
707 plants. *Biol Conserv*, 150, 76–85.

708 Wright, M.N. & Ziegler, A. (2017). ranger: A Fast Implementation of Random Forests for High  
709 Dimensional Data in C++ and R. *J Stat Softw*, 77.

710

711

712 **Supplementary information for *Six decades of losses and gains in alpha diversity of***  
713 ***European plant communities*** by Midolo, G., Clark, A. T., Chytrý, M., Essl, F., Dullinger, S.,  
714 Jandt, U., Bruelheide, H., Argagnon, O., Biurrun, I., Chiarucci, A., Čušterevska, R., De Frenne,  
715 P., De Sanctis, M., Dengler, J., Divíšek, J., Dziuba, T., Ejrnæs, R., Garbolino, E., Illa Bachs, E.,  
716 Jentsch, A., Jiménez-Alfaro, B., Lenoir, J., Moeslund, J. E., Napoleone, F., Pielech, R., Rumpf,  
717 S. B., Sanz-Zubizarreta, I., Silva, V., Svenning, J.-C., Swacha, G., Večeřa, M., Vynokurov, D.,  
718 Keil, P.  
719

## 720 **Appendix S1: Additional details on the preparation of vegetation data**

721 We calculated species richness (S) as the number of species in each plot, including subspecies  
722 and aggregates as individual species. We focused exclusively on vascular plants and excluded  
723 non-vascular plant taxa from the analysis because non-vascular plants were often not recorded.  
724 Species nomenclature was based on Euro+Med Plant-Base (Euro+Med PlantBase 2024) and that  
725 of aggregates following the EUNIS-ESy system (Chytrý et al. 2020). When counting species  
726 richness, we also included taxa identified only at the genus level. Before calculating species  
727 richness, we merged species occurrences within the same plot observation if a species was  
728 recorded in multiple vegetation layers.

729 We restricted the analysis to plots with complete information on geographical location, habitat  
730 type, plot size, and sampling year, applying specific filters based on each of these variables, as  
731 described below.

732 - ***Geographic location*** We included only plots located in Europe with available  
733 geographical coordinates. We excluded plots from Iceland, Svalbard, Russia, and Turkey.  
734 Additionally, we excluded plots with a geographic uncertainty greater than 1 km but  
735 retained plots without reported uncertainty, assuming that in a large majority of cases,  
736 their actual uncertainty is no greater than 1 km (Midolo et al. 2024; Večeřa et al. 2019).  
737 We transformed geographic coordinates to latitude and longitude in meters using  
738 ETRS89 / UTM zone 32N (EPSG:25832) projection (hereinafter, ‘northing’ and  
739 ‘easting’, respectively) and used this projection throughout the analysis. To complete the  
740 information on spatial location of all plots included in the analyses, we extracted  
741 elevation at plot location using a Digital Elevation Model with 90-m horizontal resolution  
742 from the European Space Agency (European Space Agency 2024). For the  
743 ReSurveyEurope data, we included both permanent plots (83% of the final dataset),  
744 which were resurveyed at precisely relocated sites, and quasi-permanent plots (17%),  
745 which lacked accurate relocation information. The coordinates of repeated observations  
746 for the same plot in ReSurveyEurope are not always consistent, likely due to variations in  
747 plot relocation error. Thus, to minimize potential bias in species richness interpolation  
748 during model validation, we excluded any plots in ReSurveyEurope where at least one  
749 observation was located more than 100 meters from other observations at that same plot  
750 site. This procedure resulted in the removal of 3,655 observations from 582 plots.

751 Additionally, all experimentally manipulated permanent plots were excluded from the  
752 ReSurveyEurope dataset.

753 - **Habitat types** We classified the vegetation plots into habitat types based on species  
754 composition and cover using the European Nature Information System (EUNIS) Habitat  
755 Classification expert system (Chytrý et al. 2020) (version 2021-06-01). We grouped plots  
756 into level-1 EUNIS habitat types and restricted the analyses only to plots categorized  
757 either as forest (code ‘T’), grassland (code ‘R’), scrub (code ‘S’), or wetland (code ‘Q’).  
758 We also included coastal dunes and sandy shore habitats (code ‘N1’) and classified them  
759 either as forest, grassland, or scrub depending on the physiognomy of their level-3  
760 EUNIS habitat. We discarded all plots that were not categorized in one of the habitats  
761 above, such as man-made vegetation and marine habitats. Data reported in the Danish  
762 Nature Database (Nielsen et al. 2012) (which lacks species-cover data needed for  
763 classification into EUNIS habitats by the expert system) were classified into level-1  
764 EUNIS category using the Annex I habitat conversion sheet of the same database  
765 (European Environment Agency 2023). The final selection of plots included the  
766 following number of observations for each of the habitats: 186,719 for forest (171,290 in  
767 EVA; 15,429 in ReSurveyEurope); 360,131 for grassland (309,286 in EVA; 50,845 in  
768 ReSurveyEurope); 70,334 for scrub (65,644 in EVA; 4,690 in ReSurveyEurope); 132,542  
769 for wetland (129,620 in EVA; 2,922 in ReSurveyEurope).

770 - **Plot size** We included only plots with sizes ranging from 1 to 100 m<sup>2</sup> for grasslands,  
771 scrub and wetlands, and from 100 to 1000 m<sup>2</sup> for forests to exclude outliers as well as  
772 potential mistakes of plot size reported in the datasets of EVA and  
773 ReSurveyEurope (Midolo et al. 2024). We excluded all plots with no information on plot  
774 size.

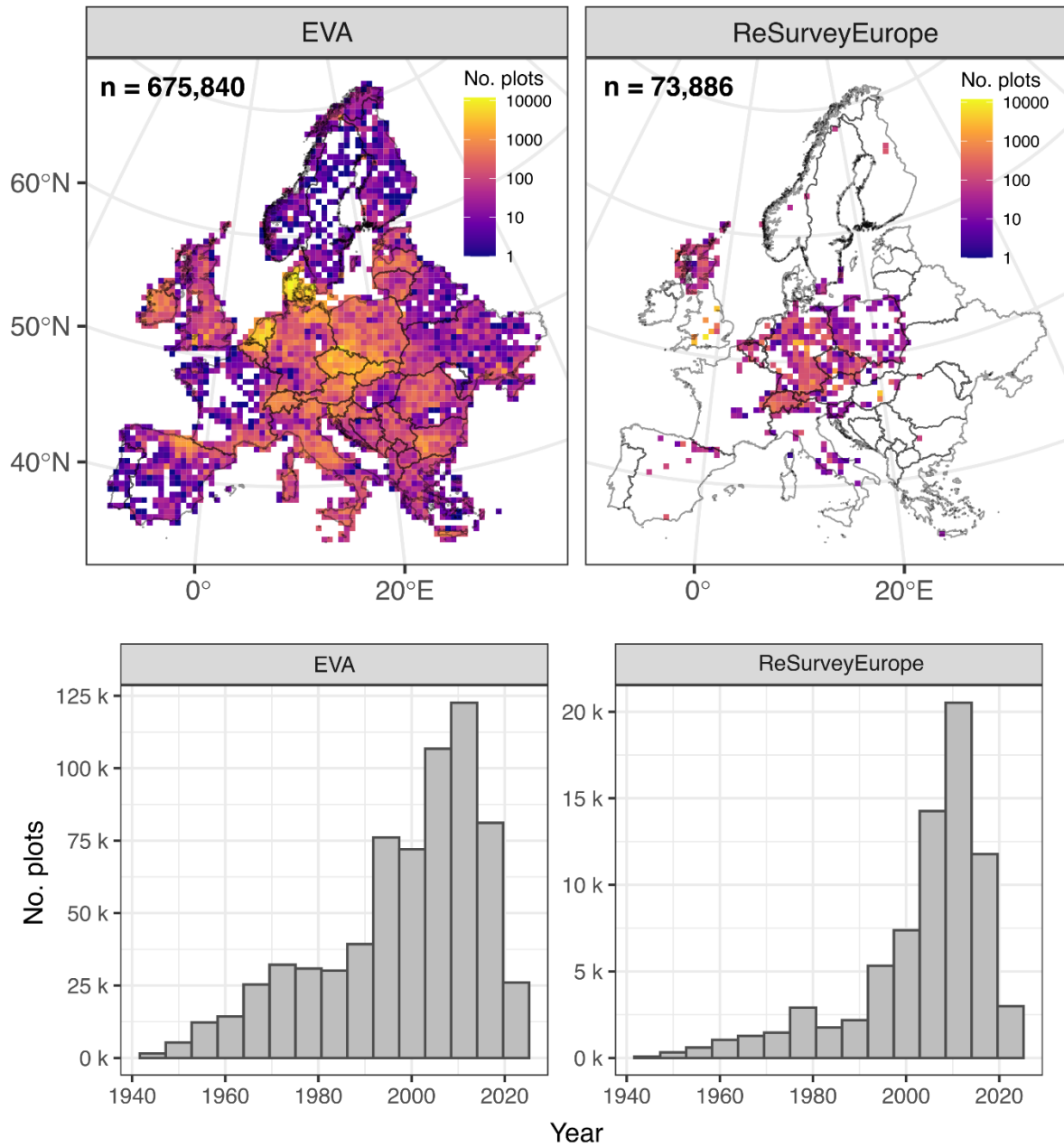
775 - **Sampling year.** We excluded plots sampled before 1945 due to a much lower number of  
776 plots compared to later periods. For model training, testing, and evaluation, we focused  
777 on plots sampled between 1945 and 2023. However, to further mitigate potential biases  
778 associated with older sampling protocols and overall fewer plots before 1960, or due to  
779 reporting lags for studies that were conducted within the last few, we restricted  
780 interpolations to plots sampled from 1960 to 2020 (see ‘Interpolation of diversity change’  
781 section). The temporal distribution of ReSurveyEurope data matched that of the EVA

782 data (Fig. S1), and we had broad temporal coverage of plots sampled in most European  
783 regions (Fig. S2-S3). Across the selected time series in the ReSurveyEurope data, the  
784 mean time span between the first and last observation was 20 years (ranging from 1 to 73  
785 years; SD = 16 years).

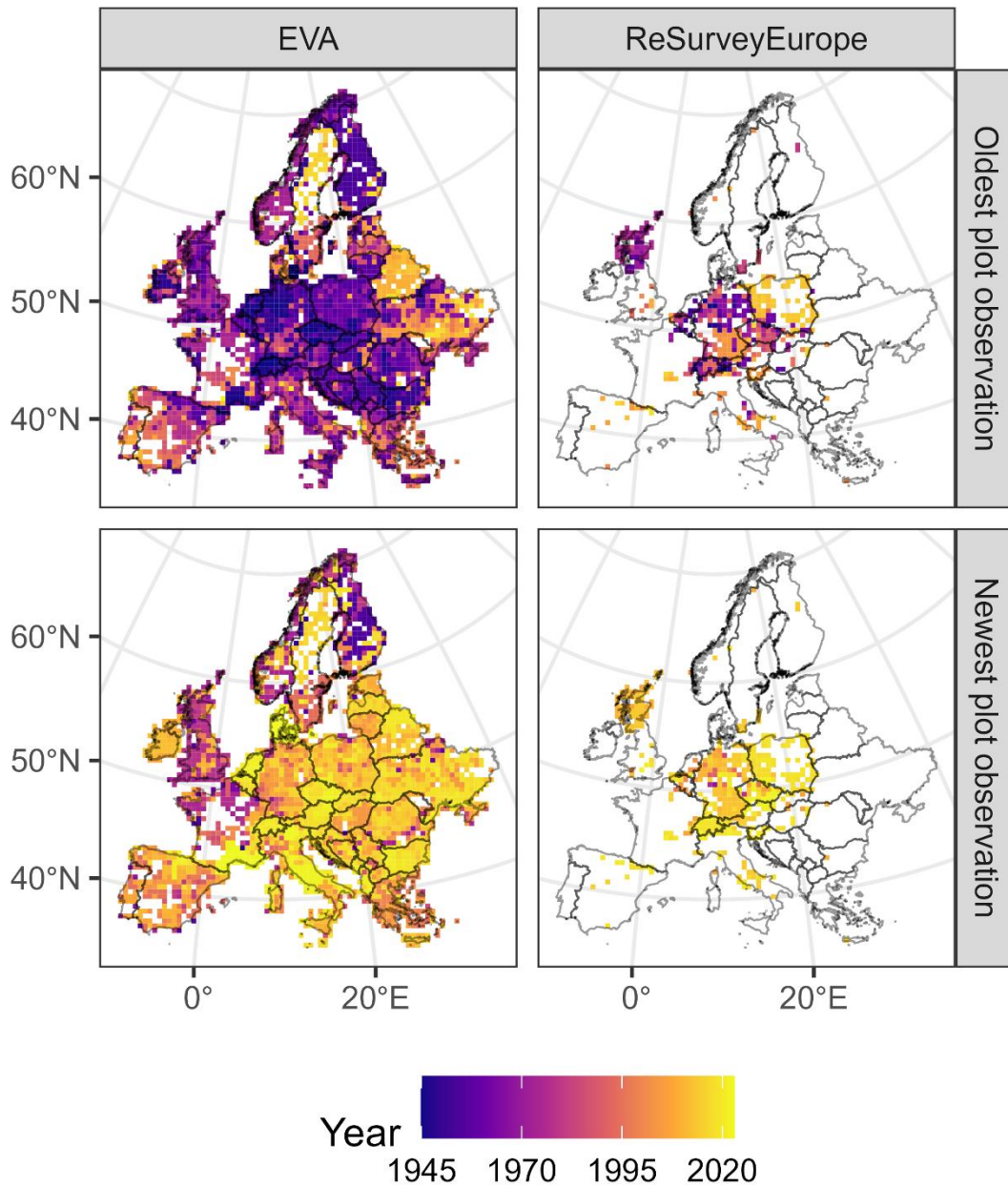
786

## 787 **References**

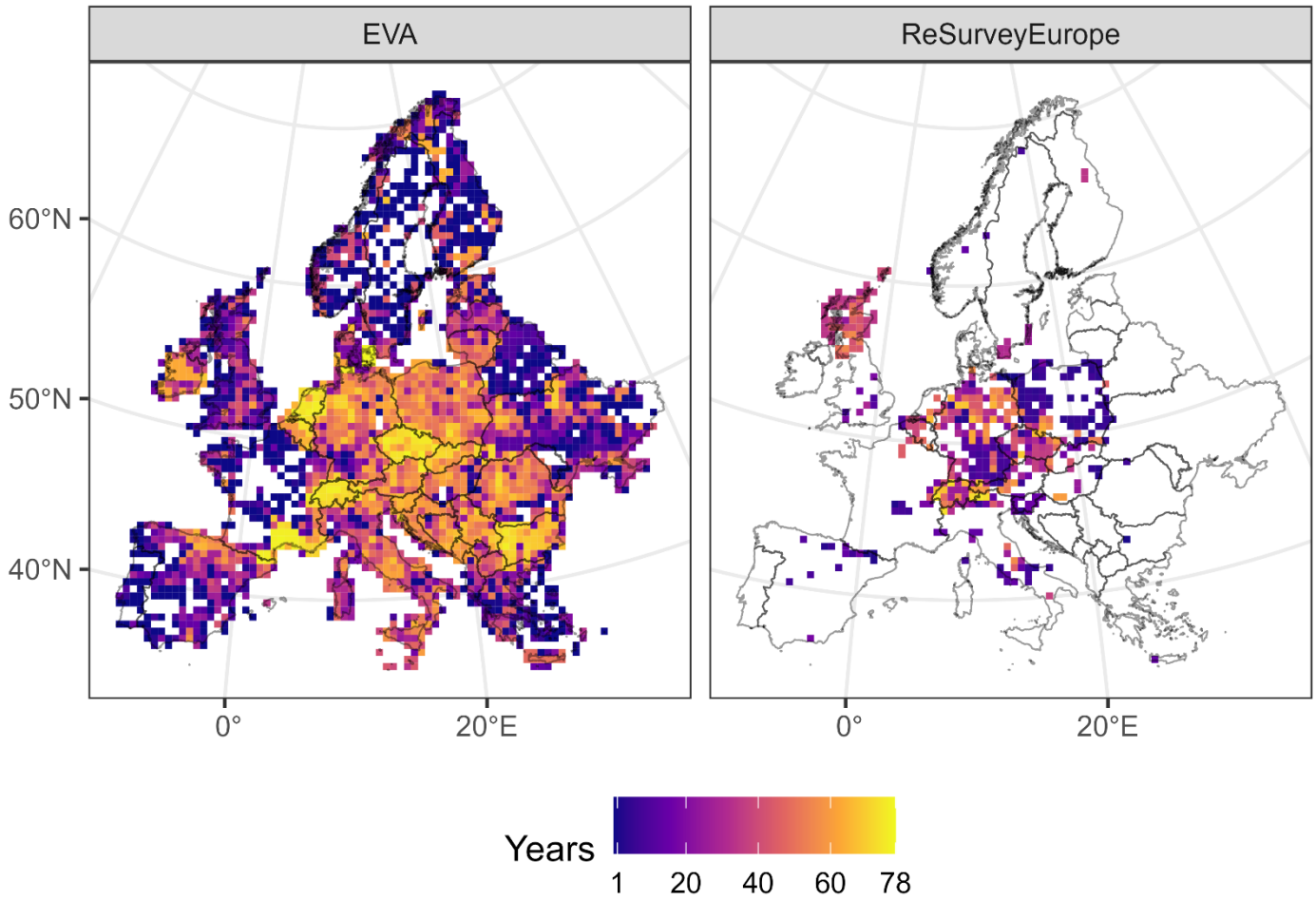
- 788 Chytrý, M., Tichý, L., Hennekens, S.M., Knollová, I., Janssen, J.A.M., Rodwell, J.S., et al.  
789 (2020). EUNIS Habitat Classification: Expert system, characteristic species combinations  
790 and distribution maps of European habitats. *Appl Veg Sci*, 23, 648–675.
- 791 Euro+Med PlantBase. (2024). Euro+Med PlantBase – the information resource for Euro-  
792 Mediterranean plant diversity. Available at: <https://www.euoplusmed.org>. Last accessed  
793 22 November 2024.
- 794 European Environment Agency. (2023). EUNIS terrestrial habitat classification 2021\_1 with  
795 crosswalks to Annex I in separate rows. 2023.
- 796 European Space Agency. (2024). Copernicus GLO-90 Digital Elevation Model. Distributed by  
797 OpenTopography. Available at: <https://doi.org/10.5069/G9028PQB>. Last accessed 12  
798 August 2024.
- 799 Midolo, G., Axmanová, I., Divíšek, J., Dřevojan, P., Lososová, Z., Večeřa, M., et al. (2024).  
800 Diversity and distribution of Raunkiær’s life forms in European vegetation. *Journal of*  
801 *Vegetation Science*, 35.
- 802 Nielsen, K., Bak, J., Bruus, M., Damgaard, C., Ejrnæs, R., Fredshavn, J., et al. (2012).  
803 NATURDATA.DK – Danish monitoring program of vegetation and chemical plant and  
804 soil data from non-forested terrestrial habitat types. *Biodiversity & Ecology*, 4, 375–375.
- 805 Večeřa, M., Divíšek, J., Lenoir, J., Jiménez-Alfaro, B., Biurrun, I., Knollová, I., et al. (2019).  
806 Alpha diversity of vascular plants in European forests. *J Biogeogr*, 46, 1919–1935.



808 **Figure S1:** Spatial (top panels;  $50 \times 50$  km resolution) and temporal (bottom panels) distribution  
 809 across plot observations of the European Vegetation Archive (EVA) and ReSurveyEurope.



810 **Figure S2:** Year of the oldest (top panels) and newest (lowest panels) plot observation located in  
 811 each grid cell ( $50 \times 50$  km resolution) across the vegetation plots of the European Vegetation  
 812 Archive (EVA) and ReSurveyEurope.

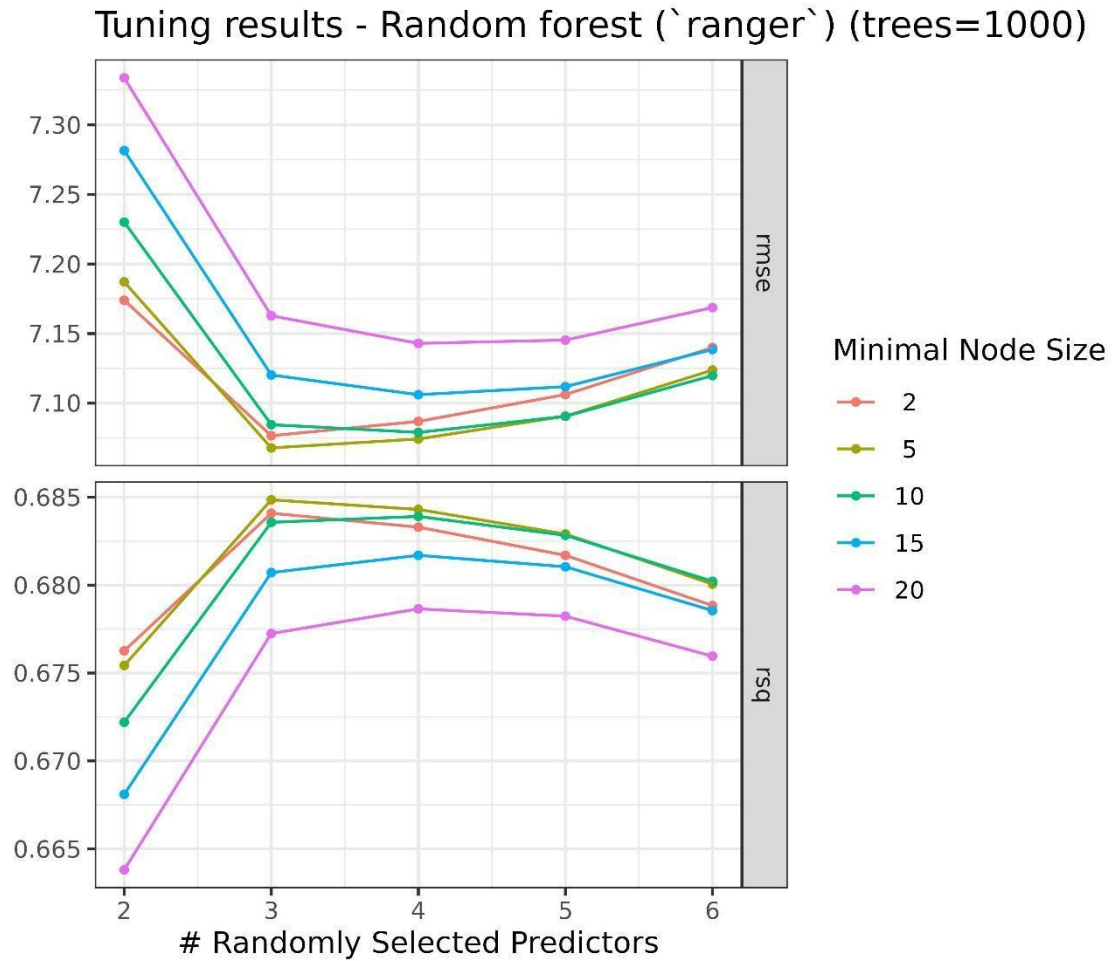


813 **Figure S3:** Temporal span (difference in years between the newest and the oldest plot  
 814 observation) located in each cell on a  $50 \times 50$  km resolution grid across the vegetation plots of  
 815 the European Vegetation Archive (EVA) and ReSurveyEurope.

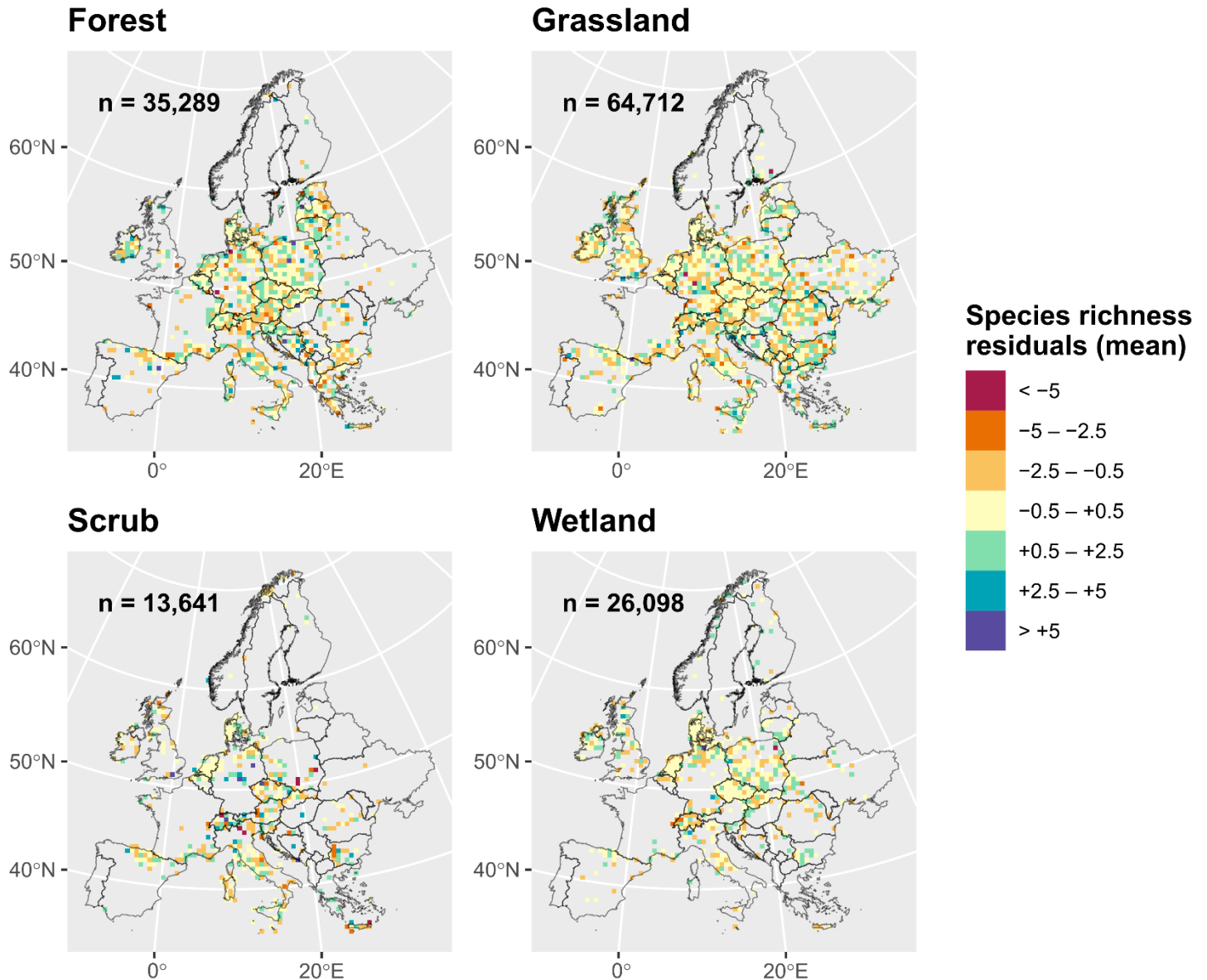
816 **Table S1:** Evaluation metrics (root mean square error, *RMSE*; coefficient of determination using  
 817 squared correlation, *rsq*) of the tested algorithms (Random Forests and XGBoost) on the full  
 818 dataset tested on 10-fold random cross validation (CV) over the training dataset (558,952) and  
 819 last fit on the testing dataset (139,740).

	<b>Random Forests</b>		<b>XGBoost</b>	
	<i>RMSE</i> (species richness)	<i>rsq</i>	<i>RMSE</i> (species richness)	<i>rsq</i>
<b>Random CV on the training set</b>	7.07 (SE: 0.0064)	0.685 (SE: 0.0005)	8.19 (SE: 0.0050)	0.580 (SE: 0.0006)
<b>Last fit on the testing set</b>	7.02	0.688	8.14	0.583

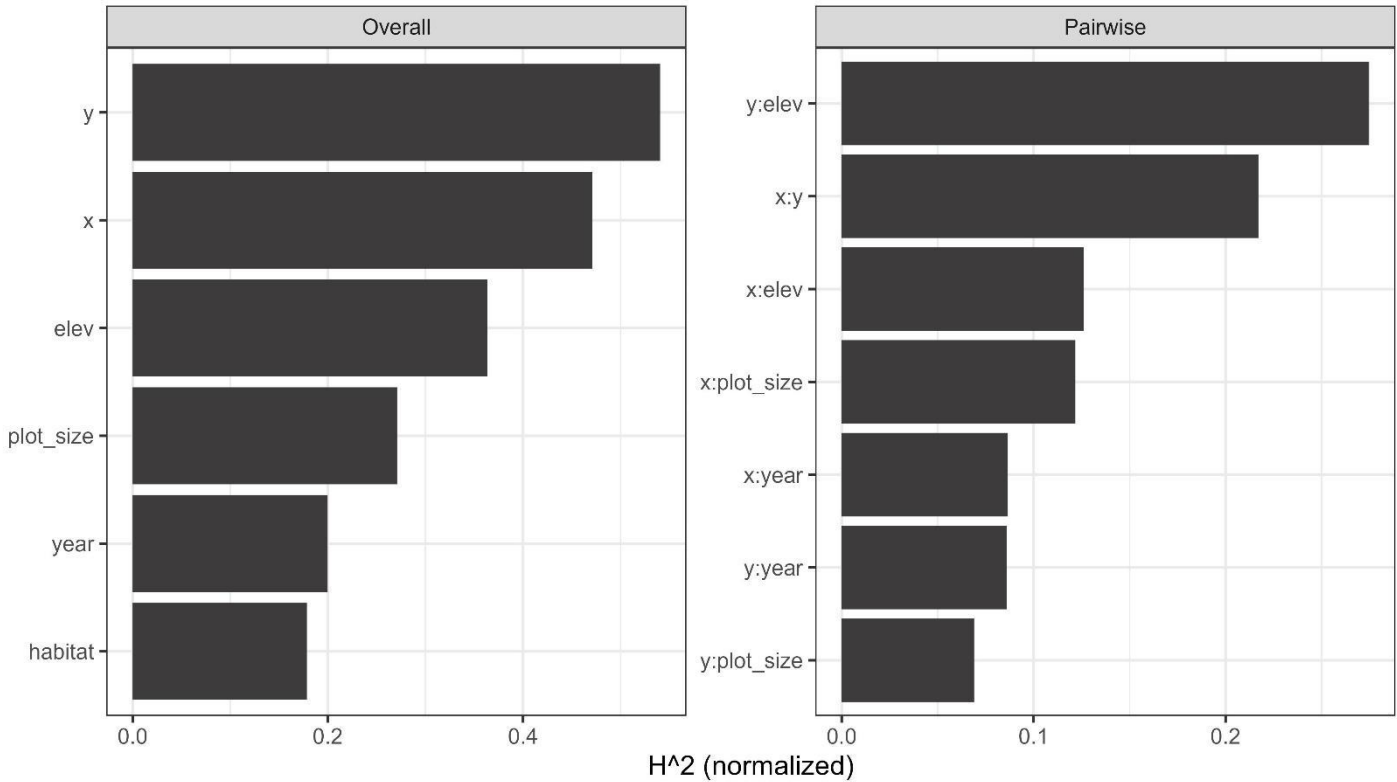
820



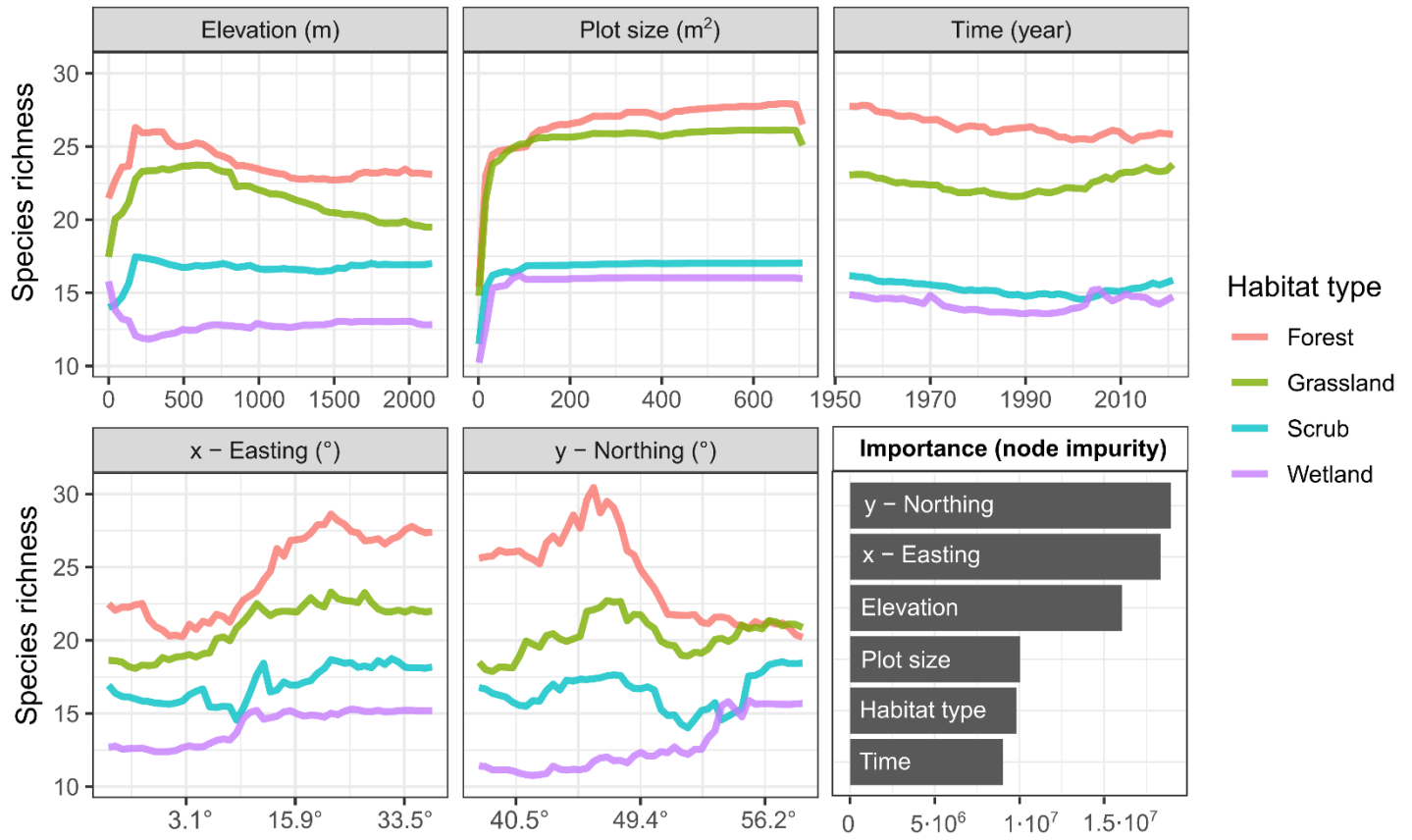
821 **Figure S4:** Hyperparameter tuning results of minimal node size and the number of randomly  
 822 selected predictors in Random Forests.



823 **Figure S5:** Spatial distribution of model residuals. The map shows the distribution of species  
 824 richness residuals (observed - predicted) across Europe from the Random Forests model  
 825 estimated over the testing data. Residuals were averaged within 50 km x 50 km grid cells for  
 826 each habitat type. Only grid cells with at least five plots are included. The number of plots (n) is  
 827 indicated within each panel. The lack of distinct geographic patterns in the residuals suggests  
 828 that the model performed similarly in predicting species richness across different regions.



829 **Figure S6:** Interaction statistic  $H^2$  describing variation explained by the interactions of terms  
 830 included in Random Forests. Overall, 71% of the total variation explained by the model was  
 831 attributable to interactions ( $H^2$  statistic = 0.71, not shown in the figure). Left panel: overall  
 832 interaction strength per feature  $H^2_j$  (= proportion of prediction variability explained by  
 833 interactions on predictor  $j$ ). Right panel: pairwise interaction strength  $H^2_{jk}$  (=proportion of joint  
 834 effect variability of predictors  $j$  and  $k$  coming from their pairwise interaction); only the top seven  
 835 interactions are shown here.

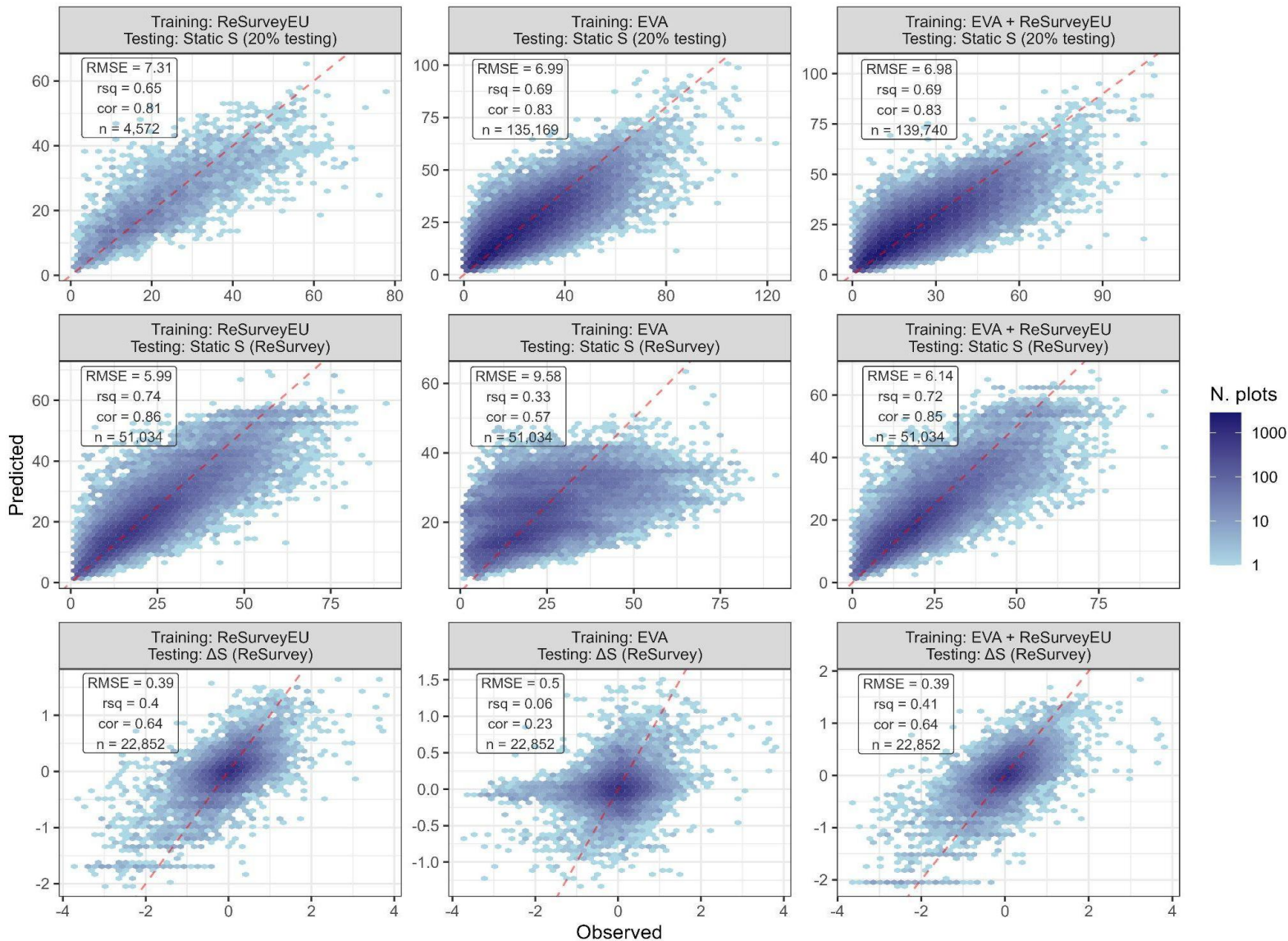


836 **Figure S7:** Partial dependence plots and variable importance (bottom-right panel) of predictors  
 837 in the Random Forests model used for species richness interpolation. Partial dependence plots  
 838 are grouped by habitat type. Easting (longitude) and northing (latitude) are originally expressed  
 839 in meters (m) (the x-axis scale is transformed to decimal degrees).

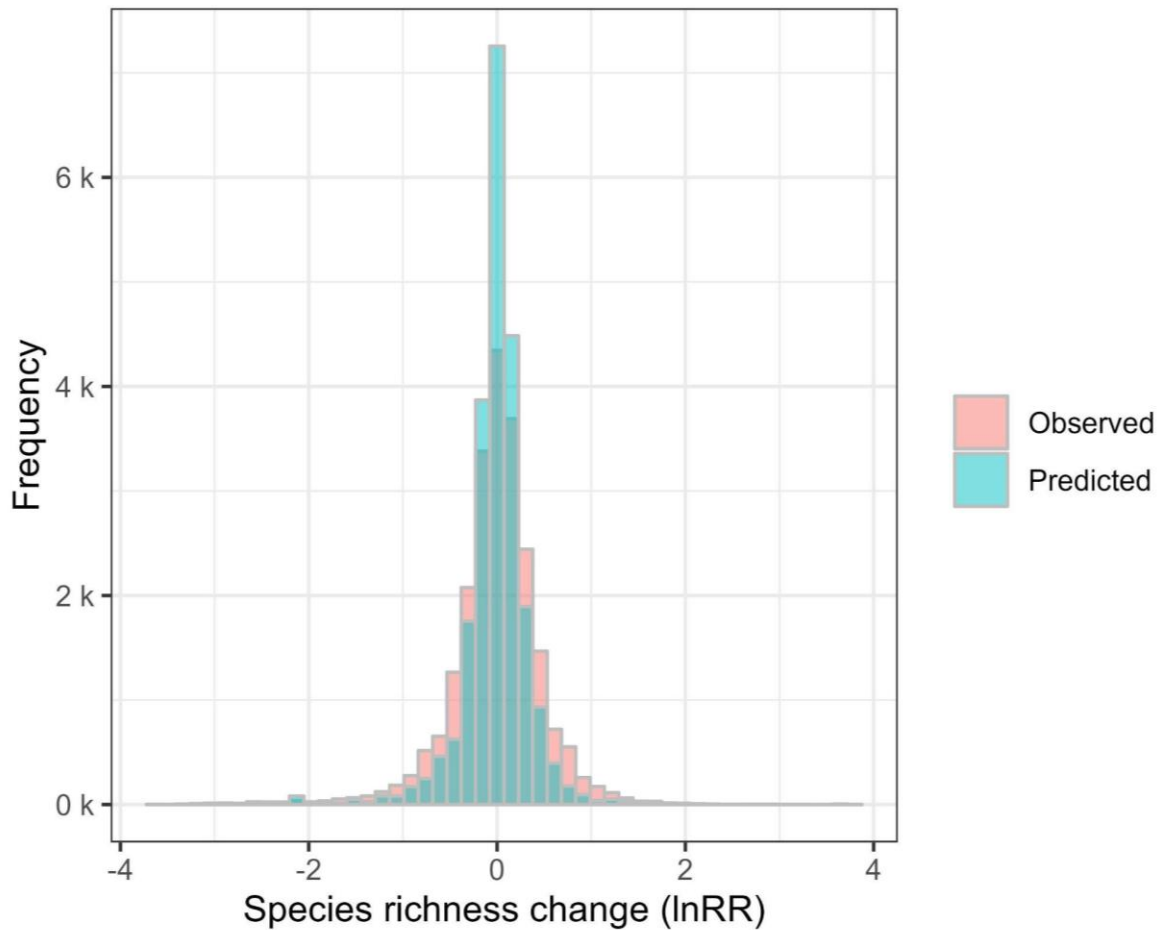
840 **Table S2:** Results of model validation trained on a static version of the ReSurveyEurope data  
 841 only. The model was fitted 100 times, with individual plots randomly selected for each time  
 842 series from the ReSurveyEurope data in each iteration. The table reports the resulting mean and  
 843 standard deviation (SD) values of various evaluation metrics (root mean square error, *RMSE*;  
 844 coefficient of determination using squared correlation, *rsq*; Pearson correlation of observed  
 845 versus predicted values; *cor*) obtained from three testing datasets. See ‘Materials and Methods’  
 846 and Fig. S8 for additional details.

	<b>RMSE</b>	<b>rsq</b>	<b>cor</b>
<b>Static <i>S</i> (20% testing)</b>	7.40 (SD: 0.1160)	0.639 (SD: 0.0096)	0.799 (SD: 0.0060)
<b>Static <i>S</i> (ReSurveyEU)</b>	5.99 (SD: 0.0244)	0.737 (SD: 0.0021)	0.858 (SD: 0.0012)
<b><math>\Delta S</math> (ReSurveyEU)</b>	0.386 (SD: 0.0018)	0.415 (SD: 0.0055)	0.645 (SD: 0.0042)

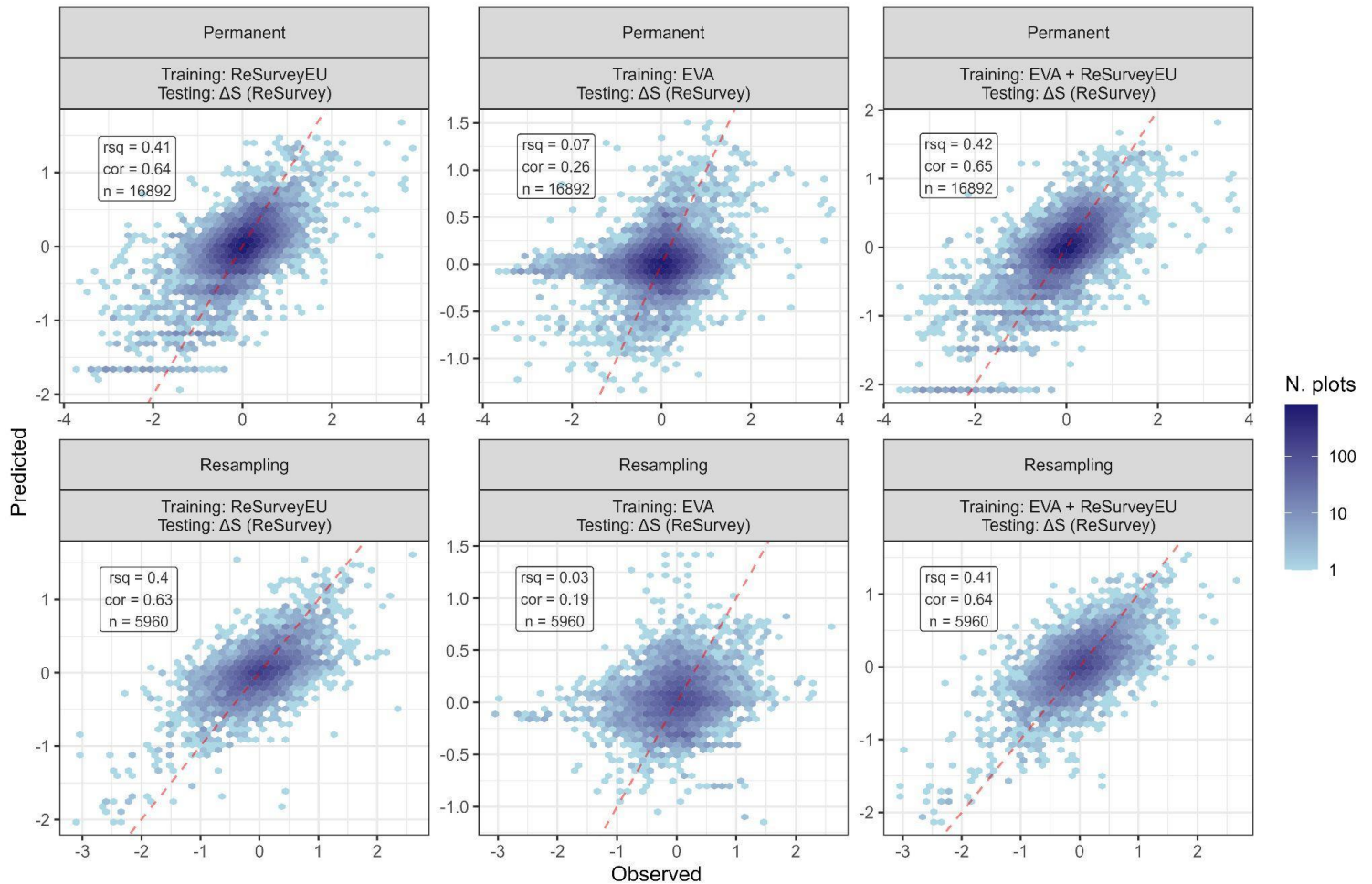
847



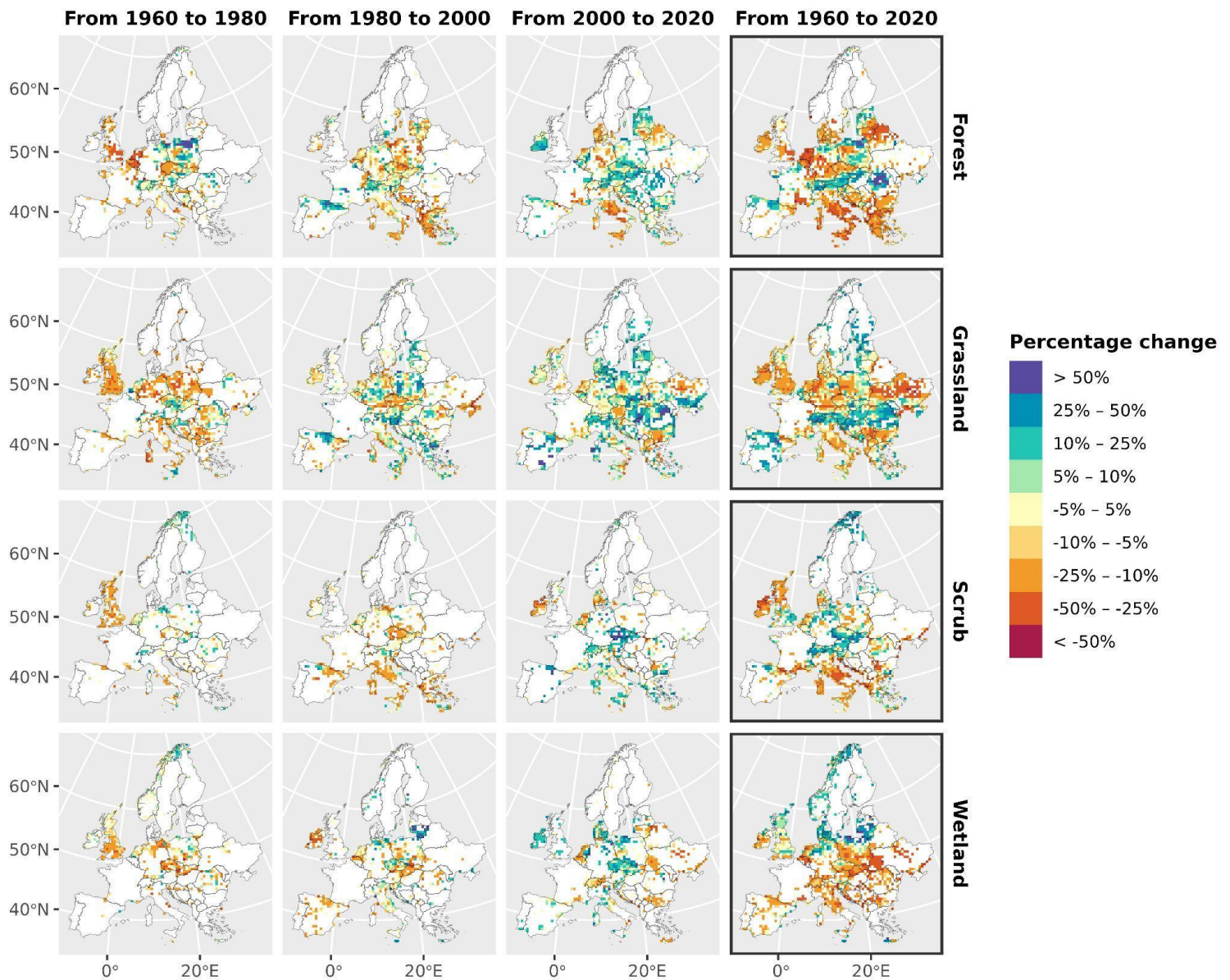
848 **Figure S8:** Validation tests for the temporal interpolation of species richness dynamics. The  
849 panel matrix reports evaluation results of observed (x-axis) vs. predicted (y-axis) species  
850 richness (static S) or its derived change ( $\Delta S$ ). Each panel includes evaluation metrics (root mean  
851 square error, *RMSE*; coefficient of determination using squared correlation, *rsq*; Pearson  
852 correlation of observed versus predicted values; *cor*) and sample size (*n*). Predictions were  
853 obtained from three models trained over different dataset combinations (columns) and tested  
854 over three different testing datasets (rows). The training data are obtained from A)  
855 ReSurveyEurope only (1<sup>st</sup> column), B) EVA only (2<sup>nd</sup> column), and C) a combination of both  
856 (3<sup>rd</sup> column), using no repeated survey. The testing dataset included 1) the 20% data from the  
857 initial split (1<sup>st</sup> row), 2) all remaining plots in ReSurveyEurope not utilized for model training  
858 (2<sup>nd</sup> row), and 3) species richness changes between the initial and final plots within each resurvey  
859 time series (3<sup>rd</sup> row). See ‘Model validation’ section in ‘Materials and Methods’ for more details.



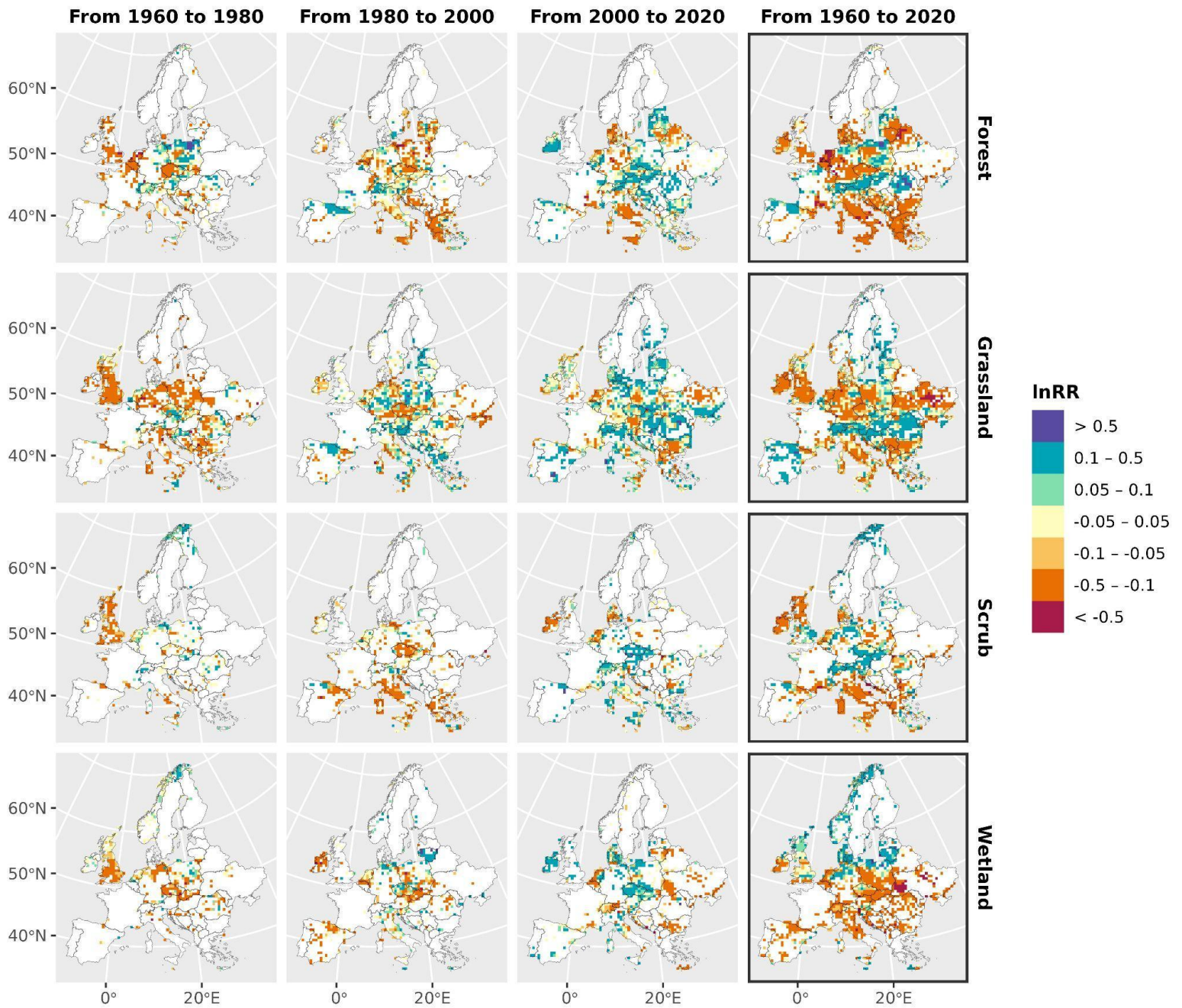
860 **Figure S9:** Interpolations tend to predict less strong changes than observed values. The  
 861 histogram compares the distribution of observed vs. predicted species richness changes across  
 862 22,852 resurvey sites. This is calculated as a log response ratio (lnRR) between the species  
 863 richness in the final plot to the one in the initial plot within each time series of ReSurveyEurope  
 864 data. Predictions were obtained from a model trained on a static version of ReSurveyEurope data  
 865 only (= using a single plot randomly selected for each time series). Same values are displayed in  
 866 the scatter plot on the bottom-left panel of Fig. S8.



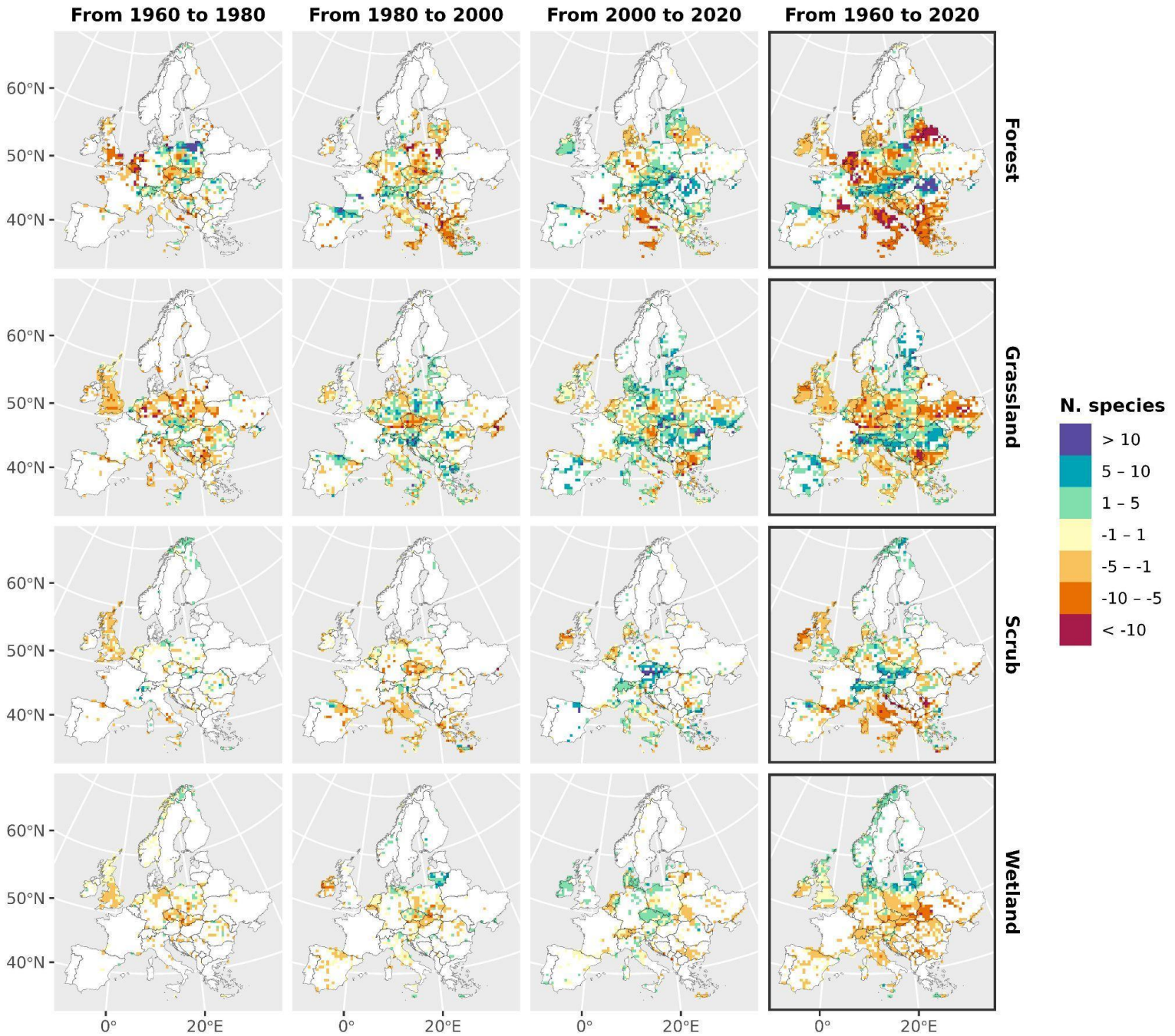
867 **Figure S10:** Validation tests for the temporal interpolation of different training datasets (see Fig.  
868 S8) comparing observed vs. predicted species richness change ( $\Delta S$ ) over ReSurveyEU data.  
869 Here, separate evaluation statistics were computed based upon the type of resurvey: either  
870 permanent plots (plots resurveyed at precisely re-located sites; first-row panels) or quasi-  
871 permanent ('Resampling') plots lacking accurate re-location (second-row panels). No significant  
872 discrepancy in model evaluation results was detected between the two re-survey methods.  
873 Species richness change is calculated as a log-response ratio (lnRR) between the species richness  
874 in the final plot to the one in the initial plot within each time series of ReSurveyEurope data.



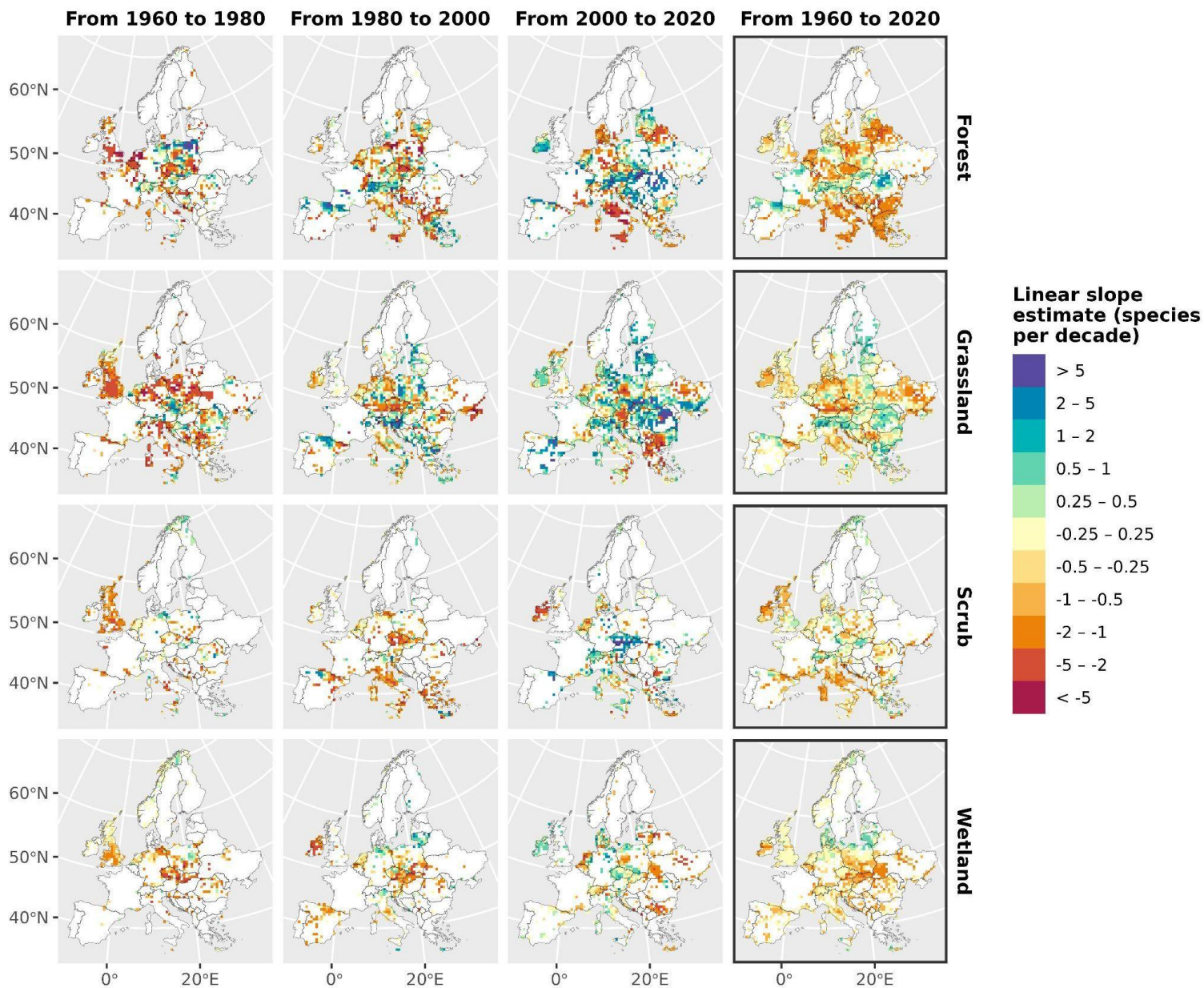
875 **Figure S11:** Geographical patterns of interpolated species richness change in Europe across main  
876 habitat types based on percentages of change (%). The maps are based on average plot-level  
877 percentage of change of species richness between two points in time for each time period, on a  
878  $50 \text{ km} \times 50 \text{ km}$  grid (as displayed in Fig. 4 in the main text). In comparison to Fig. 4, only grid  
879 cells with at least five plots sampled within each time period are displayed (i.e. number of cells  
880 varies across panels depending on data availability for a given period). To account for  
881 differences in plot sizes, we predicted species richness for each plot and year using the median  
882 plot size value for its habitat (i.e.,  $300 \text{ m}^2$  for forests,  $20 \text{ m}^2$  for grasslands,  $64 \text{ m}^2$  for scrub, and  
883  $50 \text{ m}^2$  for wetlands).



884 **Figure S12:** Geographical patterns of interpolated species richness change in Europe across main  
 885 habitat types based on *log-response ratios* ( $\ln RR$ ) in each plot. The maps are based on average  
 886 plot-level  $\ln RR$ s of species richness between two points in time for each time period, on a 50 km  
 887  $\times$  50 km grid. See Fig. S11 for additional details.



888 **Figure S13:** Geographical patterns of interpolated species richness change in Europe across main  
889 habitat types based on *absolute number of species change* in each plot. The maps are based on  
890 average plot-level number of species change between two points in time for each time period, on  
891 a 50 km × 50 km grid. See Fig. S11 for additional details.



892 **Figure S14:** Geographical patterns of interpolated species richness change in Europe across main  
 893 habitat types based on *linear slope estimates* in each plot. The maps are based on average plot-  
 894 level slope estimates obtained from linear regressions of species richness against time, on a 50  
 895 km × 50 km grid. Species change per year is expressed in decades (multiplied by 10). See Fig.  
 896 S11 for additional details.